

# Theme III: Behaviour of building structures under fire effects

Objektyp: **Group**

Zeitschrift: **IABSE congress report = Rapport du congrès AIPC = IVBH  
Kongressbericht**

Band (Jahr): **10 (1976)**

PDF erstellt am: **25.09.2024**

## **Nutzungsbedingungen**

Die ETH-Bibliothek ist Anbieterin der digitalisierten Zeitschriften. Sie besitzt keine Urheberrechte an den Inhalten der Zeitschriften. Die Rechte liegen in der Regel bei den Herausgebern.

Die auf der Plattform e-periodica veröffentlichten Dokumente stehen für nicht-kommerzielle Zwecke in Lehre und Forschung sowie für die private Nutzung frei zur Verfügung. Einzelne Dateien oder Ausdrucke aus diesem Angebot können zusammen mit diesen Nutzungsbedingungen und den korrekten Herkunftsbezeichnungen weitergegeben werden.

Das Veröffentlichen von Bildern in Print- und Online-Publikationen ist nur mit vorheriger Genehmigung der Rechteinhaber erlaubt. Die systematische Speicherung von Teilen des elektronischen Angebots auf anderen Servern bedarf ebenfalls des schriftlichen Einverständnisses der Rechteinhaber.

## **Haftungsausschluss**

Alle Angaben erfolgen ohne Gewähr für Vollständigkeit oder Richtigkeit. Es wird keine Haftung übernommen für Schäden durch die Verwendung von Informationen aus diesem Online-Angebot oder durch das Fehlen von Informationen. Dies gilt auch für Inhalte Dritter, die über dieses Angebot zugänglich sind.

### **III**

**Comportement des structures de bâtiments  
sous l'effet des incendies**

**Tragverhalten von Bauwerken unter dem  
Einfluss des Feuers**

**Behaviour of Building Structures under Fire Effects**

#### **III a**

**Effets thermiques des incendies dans les  
bâtiments**

**Thermische Auswirkungen bei  
Bauwerkbränden**

**Thermal Effects of Fires in Buildings**

#### **III b**

**Calcul et conception des structures  
métalliques ou mixtes en vue de leur résis-  
tance à l'incendie**

**Bemessung von Stahl und Verbundbau-  
werken gegen Brandeinwirkungen**

**Design of Steel and Composite Structures  
for Fire Resistance**

#### **III c**

**Calcul et conception des structures  
en béton armé ou précontraint en vue de  
leur résistance à l'incendie**

**Bemessung von Stahlbeton- und Spann-  
betonbauwerken gegen Brandeinwirkungen**

**Design of reinforced and prestressed  
concrete Structures for Fire Resistance**

Leere Seite  
Blank page  
Page vide

### IIIa

#### Comments by the Author of the Introductory Report

Remarques de l'auteur du rapport introductif

Bemerkungen des Verfassers des Einführungsberichtes

K. KAWAGOE  
Professor  
Science University of Tokyo  
Noda City, Japan

#### *Thermal Effects of Fire in Building*

The Introductory Report of Subtheme III (a) "Thermal Effects of Fires in Buildings" written by us has been issued in 1975.

Four Preliminary Reports have been presented to the Subtheme III (a) and issued before the Congress.

In the first paper "Théorie des Equivalences" by Mr.E.Absi and M.Borensztein, CEBTP, France, the calculation method to predict the temperature-time field and the thermal stress in a concrete structural element are described and some calculation results are shown.

In the second paper "Détermination par la method des éléments fines des evolutions de temperature pour les structure soumises à l'incendie" by Mr.J.C.Dotreppe and M.Hogge, Universite de Liege, Belgique, the detail of a calculation method to predict the temperature-time field in a structural element is described and an experimental result is compared with the calculated one.

In the third paper "Application of a Limit State Concept to the Performance of a Structure under Fire Conditions" by Mr.H.L. Malhotra, Fire Research Station, U.K., a new concept considered some limit state to the performance of a structure, based on the semi-probablistic approach is described.

In the fourth paper "A Differentiated Approach to Structural Fire Engineering Design" by professor O. Pettersson, Lund University, Sweden, a pure engineering design method for fire resistance of building structure which has been legally available in Sweden is described.

These four papers are connected each other and I will explain as one story mixing with our introductory report.

As Mr.Malhotra describes in his paper, "the standard temperature-time curve" for the standard fire test of building structural elements was established, and the simple relationship between the fire load density and the necessary duration of fire



exposure along the standard temperature-time curve was derived by Dr.S.H.Ingberg about 60 years ago.

Then the concept of the fire resistance design for building structure was established.

That concept was to subdivide the building effectively into "fire resisting compartments," and the building regulations and codes designated the fire duration required, depending on the occupancies and the height or the size of building and also the fire resisting capacity of structural element was determined by the results of the full scale standard fire test.

In many countries except Sweden and France, this traditional design method has been still used legally and the International Standard Fire Test Method by ISO has recently been agreed.

Over the last fifteen years the fire research has been advanced remarkably, and the people intend to use the engineering method for fire resisting design apart from the traditional way.

The first country in which a new engineering method was permitted to use legally was Sweden. Professor Pettersson describes in his paper that it is necessary to define the following four items to establish an engineering design system.

- a) the fire load characteristics,
- b) the gas temperature-time curve of the fire compartment as a function of the fire load density, the ventilation characteristics of the fire compartment,
- c) the temperature time field, and
- d) the structural behaviour and minimum load bearing capacity of the fire exposed structure for a complete process of fire development.

Our introductory report has been described along these items. Now I explain some detail of each one.

a) The survey of the fire load of several occupancies has been done in several countries. But the fire load characteristics is slightly different for each country, because the structure and the use of building are different. Therefore it is necessary to determine the fire load density in each country, whatever the survey of fire load takes much labour and time.

The explanation of fire load density has many ways, depending on the purpose, as follows,

$\frac{\text{equivalent weight of wood (Kg)}}{\text{unit floor area (m}^2\text{)}}$	(traditional)
$\frac{\text{potential heat content (Mj)}}{\text{unit floor area (m}^2\text{)}}$	(ISO)
$\frac{\text{effective heat content (Mj)}}{\text{unit interior surface area (m}^2\text{)}}$	(Sweden)
$\frac{\text{effective heat content (Mj)}}{\text{unit window area (m}^2\text{)}}$	

b) The gas temperature-time curve of a given compartment can be predicted roughly by the calculation of heat balance equation inside compartment, in which the heat release of fire load inside compartment.

In Sweden the calculated gas temperature time curve of a given compartment is taken as the heat load to the fire exposed structure, ignored "the standard temperature-time curve."

In Japan and other countries, the equivalent fire duration along the standard temperature-time curve, which temperature time area over the critical temperature of steel is same as the calculated one, is wanted to use as the heat load.

The result of the international corporative study of CIB W-14, in which eight laboratories were joined to test the model compartment fires, concluded that an experimental formula ( $t_f = kL/\sqrt{A_w A_T}$ ) as shown in Malhotra's paper could be available to use for the estimation of fire duration along the standard temperature time curve.

c) The temperature rise of steel member protected by the fire cover is not only depend on the thickness and the thermal properties of fire cover but also the heat capacity of steel member itself. It is not rational to determine only the thickness of covering material as usual designation in the codes and regulation.

In Sweden the thickness of fire cover is determined by the calculation of the heat conduction of each element exposed by each thermal load. Therefore a lot of tables and figures have been prepared, some of which are shown in Pettersson's paper.

In France the calculation method is applied legally in the concrete structural design since December 1975, which method is described in Adam's paper in subtheme III (c).

Because the theory of heat conduction has already been established, a lot of studies has been made for the prediction of temperature time field of structural elements exposed by fire.

In preliminary reports in this subtheme, Mr. Absi and Borensztein describe the calculation method used by the theory of equivalences and show some calculated results of concrete structural elements briefly. And Mr. Dotreppe and Hogge describe the detail of calculation method using the finite element one and compare an experimental result obtained from the heating of a block of concrete 18cm X 18cm with the calculated one.

In fact, in the calculation of heat balance equation in a compartment, the calculation of temperature time field of enclosed structural element is necessary. If a big computer could be used, the temperature time field could be calculated in the same time so that it is not necessary to divide b) and c).

Instead the theoretical calculation can be possible to any section of structural elements, the effect of spalling of concrete and of cracks of materials are rather difficult to insert the calculation and also the thermal properties of materials under the high temperature and the mechanism of moisture migration inside material under the high temperature are not well known, which are the problems to be solved.

d) The structural behaviour and the load bearing capacity of the fire exposed structure are the main themes of IABSE and especially in subtheme III (b) and III (c). In this subtheme III (a), Mr. Absi and Borensztein describe the calculation method of the thermal stress and the deformation used by the theory of equivalences, but the discussion of these problems is left to III (b) and (c).

For the systematize of the engineering design method based on from a) to b), many ways can be chosen. Now we look at the Swedish system as an example.

At the first, the rate of burning and the rate of heat release in a given compartment are calculated from the fire load density, the size and the geometry of compartment and the ventilation characteristics. Then the gas temperature time curve is calculated which is assumed as the heat load.

Input this heat load to the structural element, the temperature-time field inside it is calculated.

From this temperature-time field and the restraint forces, moments, thermal stress and the reduction of mechanical properties in the structural element, the load carrying capacity  $R_d$  is calculated.

Leaving these calculated results, the load effect at fire condition  $S_d$  is calculated separately.

If  $S_d$  is greater than  $R_d$ , the proposed structure is modified and recalculation is made until to obtain the satisfaction of  $S_d < R_d$ .

In Japan, tall apartment buildings of a big project was designed their fire resistance used by a similar engineering method, but it was specially permitted, not available to use any building.

Finally, the new concept of the limit state approach in fire by Mr. Malhotra is introduced. He divides the limit state into two, one is the limit state of stability which means the structural load carrying capacity under fire based on the probabilistic approach and another is the limit state of integrity which means the capacities of barrier of the compartmentation.

A similar probabilistic analysis for steel structure is presented by Dr. S.E. Magnusson in subtheme III (b).

These studies based on the probabilistic approach are only started, but the re-consideration of fire safety will become an important research subject in the fire engineering field because it would be the important basic concept of engineering design.

### Numerical Calculation of the Temperature Distribution in Hot Gas Plume from a Window

Calcul numérique de la distribution des températures dans une colonne de gaz chaud s'échappant d'une fenêtre

Numerische Berechnung der Temperaturverteilung in einer aus einem Fenster ausströmenden Heissluftsäule

YUJI HASEMI

Research Member

Building Research Institute, Ministry of Construction

Tokyo, Japan

#### 1. INTRODUCTION

In order to prevent the fire spread to upstairs through broken windows in a building, it is necessary to provide a fireproof spandrel between the windows. The estimation of its necessary height was once studied by YOKOI\*<sup>1</sup>, who conducted both dimensional analysis and small scale experiments on the behavior of the hot gas plume ejected from a window to find that the temperature distribution along its trajectory would be estimated by the normalized temperature  $\theta$  which is defined as

$$\theta \equiv \Delta\theta r_0^{5/3} / \sqrt[3]{Q^2 \theta_0 / C_p^2 \rho^2 g} \quad (1)$$

where  $\Delta\theta$ : excess temperature of the trajectory ( $^{\circ}\text{C}$ ),  $Q$ : released energy rate from window (kcal/sec),  $\theta_0$ : temperature of ambient air ( $^{\circ}\text{K}$ ),  $C$ : specific heat of air at constant pressure (kcal/kg $^{\circ}\text{K}$ ),  $r_0$ : equivalent radius of window (m) and  $\rho$ : density of hot gas (kg/m<sup>3</sup>). Fig.1 summarizes the results of the small scale experiments for various geometries of window. This simple method gives good results for many cases, but when the refractoriness of a spandrel or the interaction between the spandrel and the plume is discussed, it will be also necessary to predict the temperature dis-

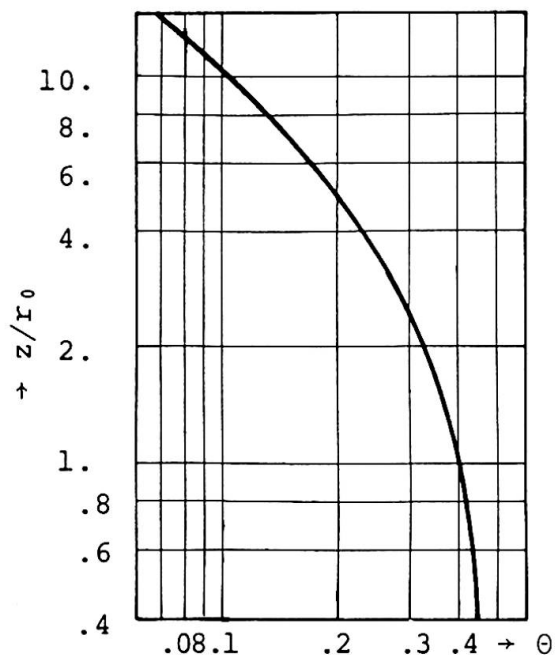


Fig.1 TEMPERATURE DISTRIBUTION ALONG THE TRAJECTORY OF HOT GAS PLUME\*<sup>1</sup>

tribution in hot gas plume, especially near the spandrel above the window.

In this paper, we introduce the calculation method by the finite difference approximation of the governing differential equations on the behavior of hot gas plume and then show a calculation result **with** an experimental one carried out under the almost similar condition to the one for the numerical calculation.

## 2. GOVERNING EQUATIONS

The governing equations of a thermally expanding or contracting turbulent motion of gas are the following set of 6\*<sup>2</sup>.

EQUATION OF MOMENTUM:

$$\frac{\partial \overline{\rho u}_i}{\partial t} + \frac{\partial \overline{\rho u}_i \overline{u}_j}{\partial x_j} \approx -\frac{\partial \overline{P}}{\partial x_i} + \frac{\partial}{\partial x_j} \{ \overline{\sigma}_{ij} + K \left( \frac{\partial \overline{\rho u}_i}{\partial x_j} + \frac{\partial \overline{\rho u}_j}{\partial x_i} \right) \} - \delta_{i3} \overline{\rho} g \quad (2)$$

where u: velocity (m/sec), P: pressure (kgm/sec<sup>2</sup>m<sup>2</sup>),  $\sigma$ : viscosity stress (kgm/sec<sup>2</sup>m<sup>2</sup>), K: eddy coefficient (m<sup>2</sup>/sec), i or j: tensor mark and  $\delta$ : KRONECKER delta. Overbarred quantities denote the time-smoothed variables. The time-smoothed velocity is given by

$$\overline{u}_i \approx \frac{\overline{\rho u}_i + K \left( \frac{\partial \overline{\rho}}{\partial x} \right)_i}{\overline{\rho}} \quad (3)$$

EQUATION OF CONTINUITY:

As the time-smoothed density is obtained from the equation of state in our calculation scheme, the equation of continuity should be transformed to the POISSON type equation for  $\overline{P}$ . This equation is obtained by substituting the equation of momentum into the natural form of continuity equation  $\partial \overline{\rho} / \partial t + (\partial \overline{\rho u} / \partial x)_i = 0$ .

$$\frac{\partial^2 \overline{P}}{\partial x_i^2} \approx \frac{\partial^2 \overline{\rho}}{\partial t^2} + \frac{\partial^2}{\partial x_i \partial x_j} \{ \overline{\sigma}_{ij} + K \left( \frac{\partial \overline{\rho u}_i}{\partial x_j} + \frac{\partial \overline{\rho u}_j}{\partial x_i} \right) - \overline{\rho u}_i \overline{u}_j \} - g \frac{\partial \overline{\rho}}{\partial x_3} \quad (4)$$

CONSERVATION EQUATION OF ENERGY:

$$\overline{\rho} \frac{\partial \overline{h}}{\partial t} + \frac{\partial \overline{\rho u}_i \overline{h}}{\partial x_i} \approx \frac{\partial}{\partial x_i} \left( \kappa \frac{\partial \overline{T}}{\partial x_i} + K \frac{\partial \overline{h}}{\partial x_i} \right) + \overline{Q} + h \frac{\partial \overline{\rho u}_i}{\partial x_i} \quad (5)$$

where h: enthalpy of air (kcal/kg),  $\kappa$ : thermal conductivity (kcal/sec m) and Q: generation rate of heat (kcal/sec m<sup>3</sup>). The dissipation of kinetic energy is ignored for its minor role in the conservation of energy.

DEFINITION OF EDDY COEFFICIENT:

PRANDTL's dimensional relationship is applied to the modeling of eddy coefficient. In this model, eddy coefficient is given by

$$K \approx \sqrt{\overline{q}} \ell \quad (6)$$

where the mixing length ' $\ell$ ' may be determined geometrically and the turbulent energy is given from the conservation equation for it.

$$\frac{\partial \overline{\rho q}}{\partial t} + \frac{\partial \overline{\rho u}_i \overline{q}}{\partial x_i} \approx \frac{\partial}{\partial x_i} \left( \overline{\rho} K \frac{\partial \overline{q}}{\partial x_i} + \mu \frac{\partial \overline{q}}{\partial x_i} \right) + K \frac{\partial \overline{\rho}}{\partial x_3} g - \overline{\rho} \epsilon + K \left( \frac{\partial \overline{\rho u}_i}{\partial x_j} + \frac{\partial \overline{\rho u}_j}{\partial x_i} \right) \frac{\partial \overline{u}_j}{\partial x_i} \quad (7)$$

where  $\mu$ : dynamic viscosity (kg/sec m) and  $\epsilon$ : turbulent energy decay rate (m<sup>2</sup>/sec<sup>3</sup>).



## EQUATION OF STATE:

The change or variation of the pressure in fire is usually so small that the equation of state may be approximated correctly by

$$\bar{\rho} \approx \frac{P_0}{RT} \quad (8)$$

where  $P_0$ :referential pressure(kgm/sec<sup>2</sup>m<sup>2</sup>), R:gas constant and T: absolute temperature of air(°K).

3. OUTLINE OF THE CALCULATION METHOD

The governing equations above introduced are of course so complicated for an analytical solution that we solve them simultaneously in a numerical manner. However, because we do not have enough space to describe everything about the calculation method, we present the outline of the finite difference calculation method which is detailed in REF.2.

In our numerical code, the unsteady equations (2), (3) and (7) are transformed into explicit finite difference equations, whilst the POISSON type equation for the pressure (4) is solved by an iterative method such as Over-Relaxation method. For the finite difference calculation of the spacially differentiated terms, the Cell Model in which the physical variables are arranged by the way as shown in Fig.2 is used. A stable marching of the unsteady calculation is achieved only when the finite increment of time satisfies the following criterion which is known as COURANT-FRIEDRICHS-LEWY condition.

$$\Delta t < \frac{1}{\left(\frac{3}{4} |\bar{u}_i / \Delta x_i|\right)_{\max}} \quad (9)$$

Then, the finite difference equations for (2)~(8) are solved unsteadily by the procedure as shown in Fig.3.

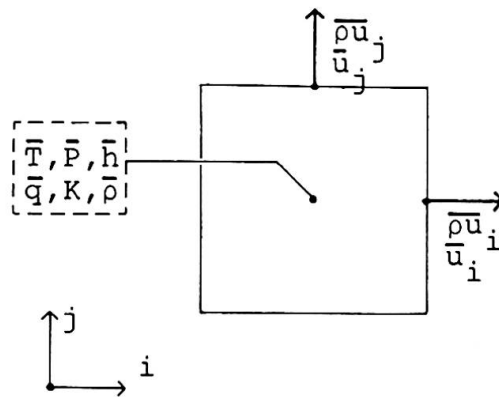


Fig.2 GRID ARRANGEMENT  
IN CELL MODEL

4. CALCULATION OF THE TEMPERATURE DISTRIBUTION IN HOT GAS PLUME

Now, we apply the calculation method above introduced to the estimation of the temperature distribution of a hot gas plume ejected from a broken window.

It was suggested by YOKOI\*<sup>1</sup> on the basis of the results of his small scale experiments that the hot gas plume from a wide opening would close to the wall or spandrel above it to be a possible cause of the fire spread to upstairs. This phenomenon which may be interpreted by the COANDA effect was also observed in the full scale experiment conducted recently by KAWAGOE et al\*<sup>3</sup>. Such a phenomenon seems to be represented pertinently in a two-dimensional calculation, because we may conceptually replace a wide opening by a two-dimensional one without bringing any serious problem.

In this paper, we make a numerical calculation of the hot gas plume under the conditions which are determined according to KAWA-

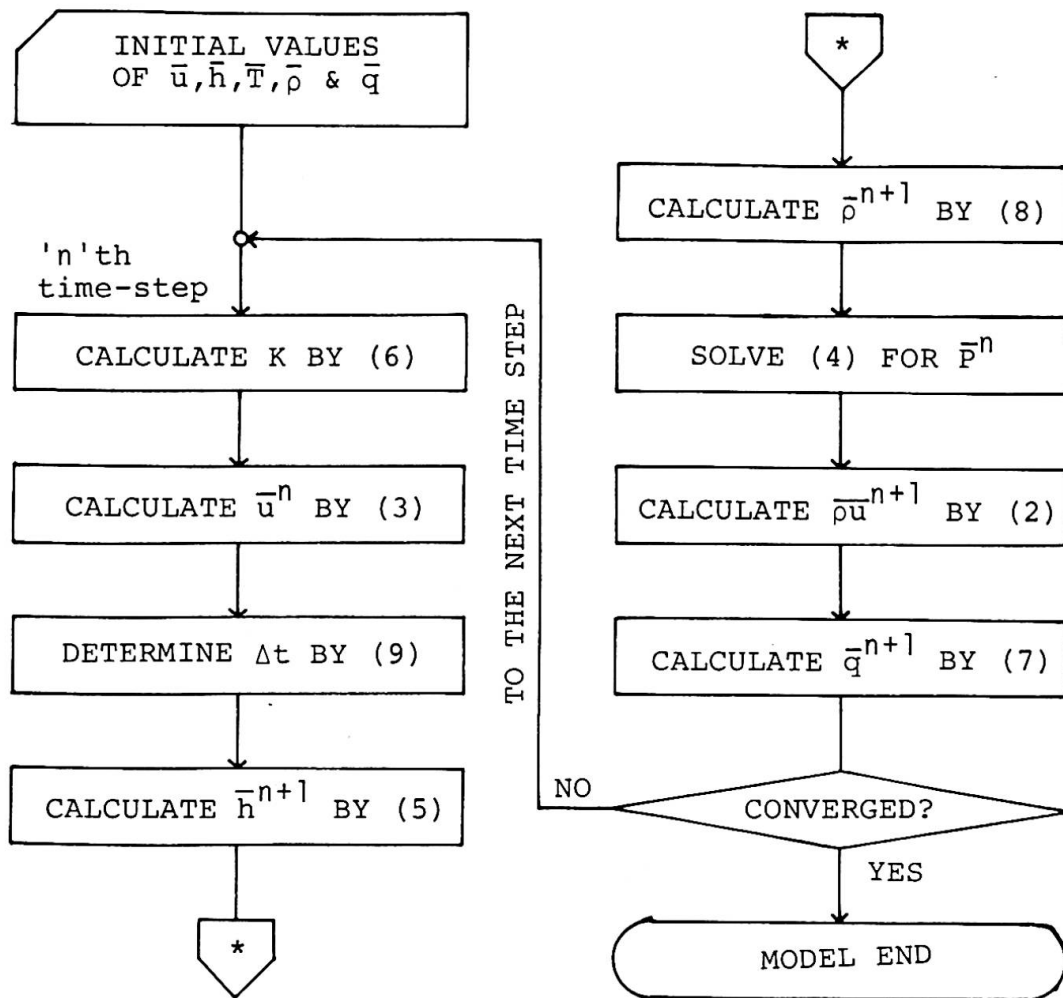


Fig.3 OUTLINE OF THE UNSTEADY CALCULATION PROCEDURE

GOE's experiment as shown in Tab.1 and then compare the calculation result with the experimental one. Among these conditions for the calculation, the height of neutral plane and the distribution of the mixing length are determined empirically and the spouting velocity is estimated by YOKOI's equation.

Tab.1 CONDITIONS FOR THE NUMERICAL CALCULATION

TEMPERATURE OF HOT GAS PLUME AT OPENING	900°C
TEMPERATURE IN UPSTAIRS ROOM	100°C
TEMPERATURE OF AMBIENT AIR	30°C
MASS FLUX RATE OF PLUME AT OPENING	$\rho U = \sqrt{2gh''(\rho_0 - \rho)}$ $\rho_0$ : density of ambient air $h''$ : height from neutral plane
MIXING LENGTH	$l = 0.4y, l_{\max} = 0.2H$ $y$ : distance from boundary $H$ : height of building

In Fig.4 are superimposed the calculated isotherms on the temperature field generated from the experiment. Although the discrepancy between the calculated and experimental distributions near the opening of the fire compartment is considerably great, the phenomenon above mentioned which may be a cause of the fire spread to upstairs is represented pertinently in the calculation result.

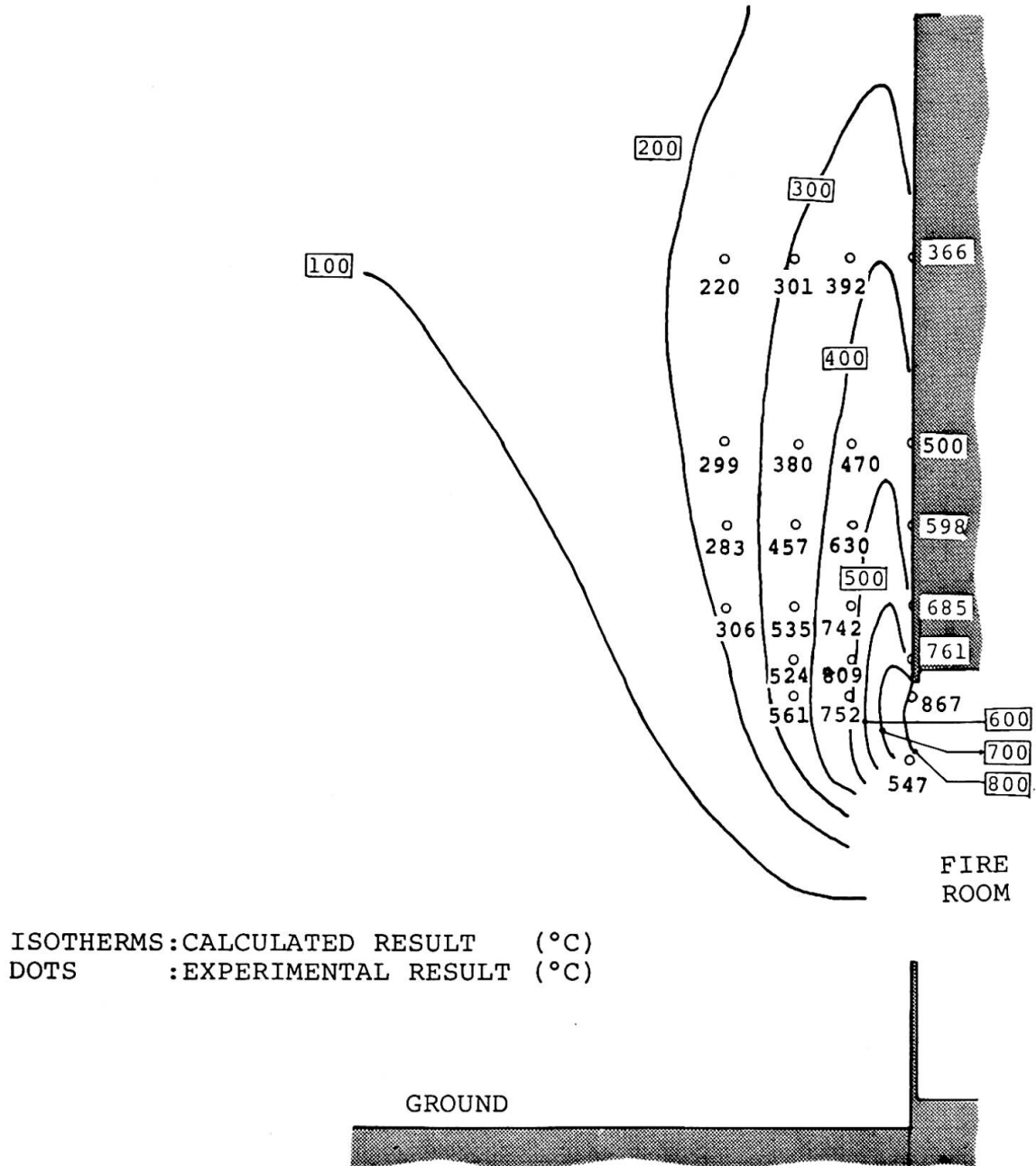


Fig.4 TEMPERATURE DISTRIBUTION IN HOT GAS PLUME FROM A WINDOW  
 (COMPARISON OF CALCULATED AND EXPERIMENTAL RESULTS)

## 5. CONCLUSIONS

The temperature distribution in two-dimensional hot gas plume was calculated as an application of the prediction method. The use of a large EDPS will permit also a three-dimensional calculation, because the calculation method for the three-dimensional case does



not differ basically from the one for the two-dimensional case which is introduced in this paper. Though some problems such as the calculation of the flame radiation are left as future subjects, we can utilize such a calculated temperature distribution for designing the height or refractoriness of a spandrel from the view point of fire safety.

#### REFERENCES

- 1) YOKOI,S: "Study on the Prevention of Fire-Spread Caused by Hot Upward Current",BRI Research Report,No.34,1960.
- 2) HASEMI,Y: "Numerical Simulation of Fire Phenomena and its Application",BRI Research Paper,No.66,1976.
- 3) KAWAGOE,K et al:"Report on '502' Fire Experiment",Science Univ. of Tokyo,1975.

#### SUMMARY

This paper presents a method for the numerical calculation of the temperature distribution in a hot gas plume from a window. The calculation is given for a two-dimensional window and also compared with experimental results. Calculation and experiments show a good agreement.

#### RESUME

Cet article présente une méthode numérique pour calculer la distribution des températures dans une colonne de gaz chaud s'échappant d'une fenêtre. Le calcul est présenté pour une fenêtre à deux dimensions et est aussi comparé avec des résultats expérimentaux. La concordance entre le calcul et l'expérience est bonne.

#### ZUSAMMENFASSUNG

Der Autor beschreibt ein numerisches Verfahren zur Berechnung der Temperaturverteilung in einer aus einem Fenster ausströmenden Heissluftsäule. Die Berechnung wird für ein zweidimensionales Fenster vorgelegt und mit Versuchsergebnissen verglichen. Die Uebereinstimmung zwischen Berechnung und Versuch ist gut.

### Design of Tall Apartment Buildings for Fire Resistance

Conception de bâtiments d'habitation hauts en vue de leur résistance à l'incendie

Entwurf von hohen Wohnhäusern in bezug auf Brandeinwirkungen

KOJI IIZUKA

Chief Research Engineer

Technical Research Laboratory, Takenaka Komuten Co. Ltd.

Tokyo, Japan

AKIO KODAIRA

Research Engineer

Technical Research Laboratory, Takenaka Komuten Co. Ltd.

Tokyo, Japan

The existing Japanese building codes for fireproof constructions prescribe the fire endurance of the individual structural elements, such as beams, columns, floors and so on, without concerning the fire properties and structural features of buildings. Buildings have been designed against fire according to these codes. However, researches on the fire properties in compartments and the behaviour of steel structures under fire have recently been carried out and made the design of fireproof constructions possible by engineering methods.

This paper discusses the method and the results of the fireproofing design of the Ashiyahama Housing Project currently under construction. The Ashiyahama Housing project consists of many multistoried buildings as shown in Photo 1 and the dwellings totaled 3384.

The fireproofing design system used on this project is illustrated in Fig.1, and the following procedure was applied:

- 1) Fire compartments were allocated as shown in Fig. 2.
- 2) Fire loads were estimated from the quantity and the quality of the combustible materials for individual fire compartments.
- 3) Using a monograph, the equivalent fire duration time of dwelling unit was obtained from the fire load, floor factor, temperature factor and others. The equivalent fire duration time of public floor was determined by taking into account the fire load and burning phenomenon in the open space.
- 4) If the fire was not to spread to the adjoining fire compartments, then advance to the next step.
- 5) Using a computer program, allowable temperature of the steel frame was calculated from dead load, live load, thermal expansion and deterioration of steel members at elevated temperature. Shown as example, Fig.3 represents the joint displacement according to only thermal expansion and Fig.4 shows the distribution of bending moment that is due to the ordinary design load and the thermal expansion.

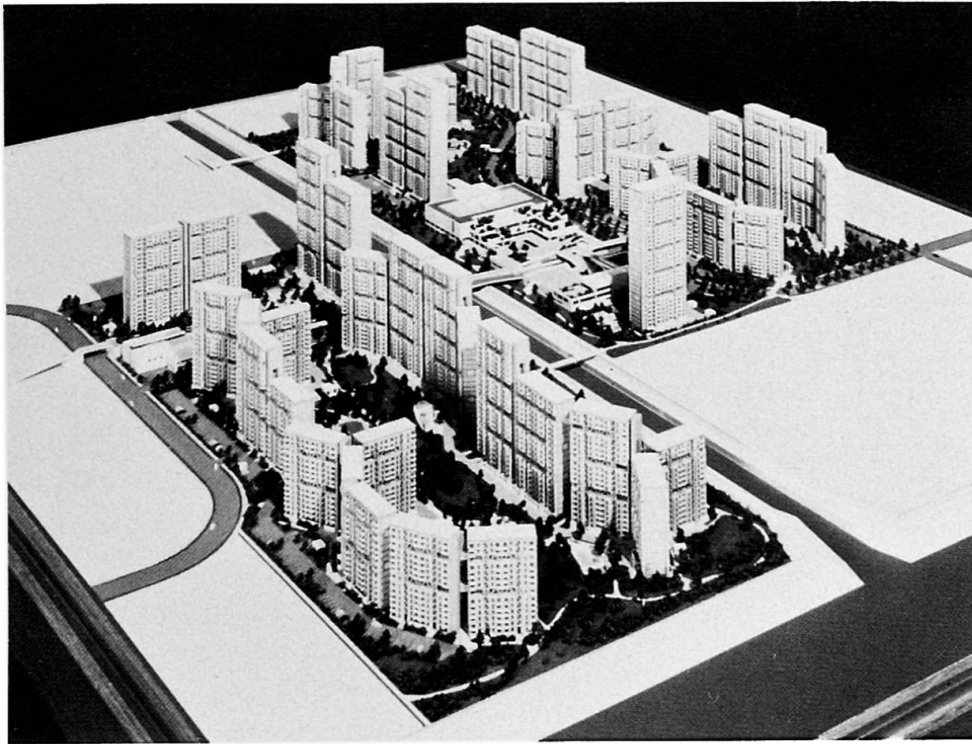


Photo 1: The bird's-eye view of the Ashiyahama Housing Project. (model)

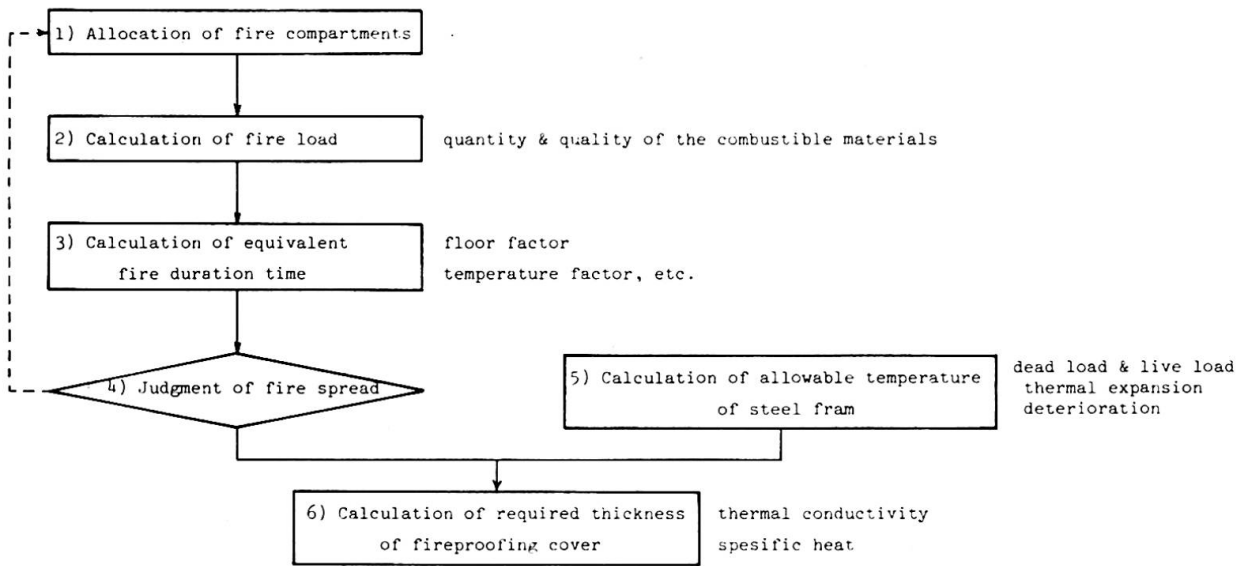


Fig. 1: The fire proofing design system

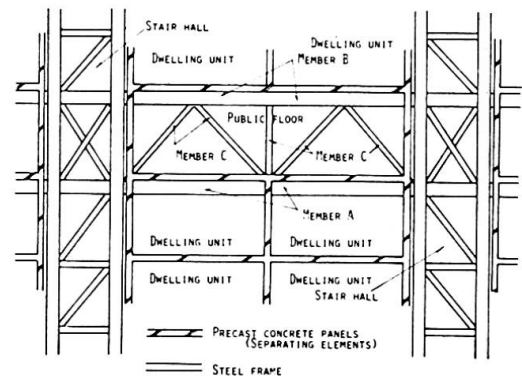


Fig. 2: The fire compartment and steel frame

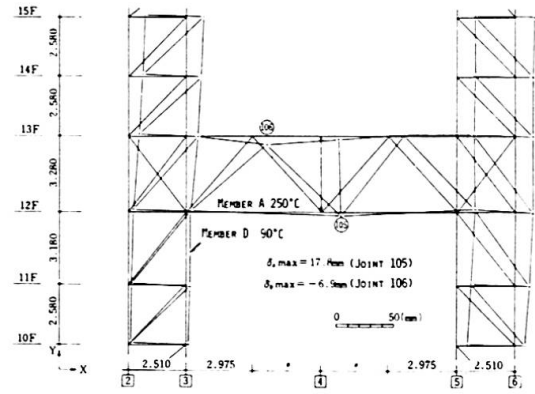


Fig. 3: Joint displacement according to only thermal expansion

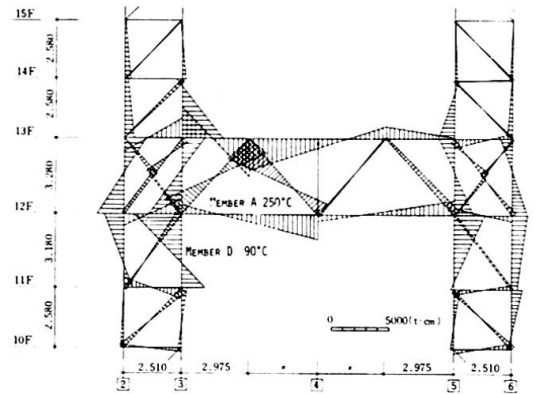


Fig. 4: Distribution of bending moment according to the ordinary design load and the thermal expansion

Fire compartments	Fire load (Kg/m <sup>2</sup> )	Equivalent fire duration time (min.)	steel members in compartment	allowable temperature of steel members (°C)	Required thickness of fireproofing cover* (mm)
Dwelling unit	60	90	A	250	45
Public floor	15	30	B	200	15
			C	100	15**
Stair hall	0		others		0

\* Sprayed asbestos.

\*\* This value was determined by taking into account the heating condition and birning phenomenon in the open space.

Table 1: Results of the fireproofing design

- 6) The need for some fireproofing cover was realized by which the temperature rise of steel member could be kept below the allowable temperature after heating for equivalent fire duration time along the standard time-temperature curve. The required thicknesses of the fireproofing cover for members named A, B and C were calculated. It was found that other members did not require fireproofing cover.

These results are tabulated in Table 1.

Adopting the fireproofing design in this project despite the current building codes, structural safety against fire was secured and economical design was established.

The fireproofing design system adopted in this project can be applied, without modification, to such design of other buildings.

#### References

1. Kawagoe, K., and Sekine, T., "Estimation of Fire Temperature-Time Curve in Rooms", Building Research Institute of Japan, Research Paper No.11, No.17, No.29
2. Saito, H., "Research on the Fire Resistance of Steel Beam", Building Research Institute of Japan, Research Paper No. 31, 1968
3. Kawagoe, K., "System Design for Fire Safety", Proceedings of the International Conference on Planning and Design of Tall Buildings, Vol.Ib,1972
4. Kawagoe, K., and Saito, H., "Thermal Effects of Fire in Buildings", Introductory Report of Tenth Congress of IABSE, 1976

#### SUMMARY

This paper discusses the method and results of the fireproofing design for the Ashiyahama Housing Project currently under construction. By adopting the fireproofing design in this project, without restriction of the existing Japanese building codes for fireproofing construction, the structural safety against fire was secured and economical design was satisfied.

#### RESUME

Cette étude discute la méthode et les résultats du calcul et de la conception du quartier d'habitation d'Ashiyahama en vue de la résistance à l'incendie. L'adoption de cette méthode qui n'est pas en contradiction avec la réglementation actuelle japonaise en la matière a permis d'assurer la sécurité structurale contre l'incendie et de réaliser un projet économique.

#### ZUSAMMENFASSUNG

Dieser Artikel erörtert die Methoden und Ergebnisse des Entwurfs in bezug auf Brandeinwirkungen für das derzeit im Bau stehende Ashiyahama Wohnbauprojekt. Die für dieses Projekt herangezogene Methode gewährleistet einen ausreichenden Brandschutz, ist zudem wirtschaftlich und entspricht in allen Punkten den bestehenden japanischen Vorschriften für brandsichere Bauten.

**Calcul automatique de la résistance au feu des ossatures métalliques**

Automatische Berechnung des Feuerwiderstandes von Stahlbauten

Automatic Computation of Fire Resistance of Steel Structures

**A. MASSONNET**

Ingénieur Civil des Constructions

**J.C. DOTREPPE**

Chargé de Recherches au F.N.R.S.

Université de Liège

Liège, Belgique

**1. INTRODUCTION.**

Dans cet article, on présente un code de calcul permettant d'évaluer, de manière automatique, la résistance au feu des ossatures métalliques protégées et non protégées.

Le comportement au feu des structures métalliques présente un certain nombre de caractéristiques qui permettent l'utilisation de techniques de calcul particulières, analogues à celles utilisées pour le calcul à la ruine des structures métalliques ordinaires. Le procédé s'apparente aux méthodes de l'analyse limite des ossatures en acier doux, basées sur le concept de rotule plastique.

Le calcul de l'évolution de la température dans les éléments se fait de manière simple en admettant que la température est uniforme sur la section droite.

**2. CALCUL DE L'ELEVATION DE LA TEMPERATURE DANS LES PROFILS.**

Dans le Rapport Préliminaire [5], on a indiqué la technique utilisée pour le calcul de l'évolution de la température dans les éléments soumis à l'incendie. En règle générale, il s'agit de résoudre l'équation de Fourier, assortie de conditions aux limites de différents types.

Dans le cas d'un profilé en acier, le calcul des températures peut être fortement simplifié, par suite des valeurs élevées de la conductivité thermique  $\lambda$ . L'hypothèse simplificatrice consiste à admettre que la température du profilé est uniforme. Cette hypothèse est plausible dans le cas des profilés ordinaires en double T, par suite de la minceur de l'âme et des semelles et de la grande surface exposée au feu.

**2.1. Cas d'un profilé non protégé.**

Soit un élément de volume  $dV$  soumis à un flux de chaleur  $Q$ . Le bilan calorifique de cet élément s'écrit (cf. figure 1) :

$$Q \, dA = c \rho \frac{\partial \theta}{\partial t} dV \quad (1)$$

où  $dA$  est la surface extérieure de l'élément.

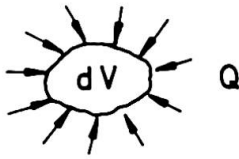


Figure 1

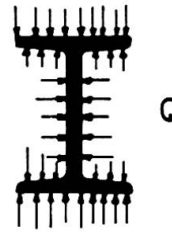


Figure 2

Le même bilan peut s'écrire en ce qui concerne un profilé métallique non protégé, puisqu'on suppose que les calories absorbées se répartissent instantanément de manière uniforme dans toute la masse de l'acier (figure 2). L'équation (1) s'écrit alors :

$$Q \frac{U}{F} = c \rho \frac{\partial \theta}{\partial t} \quad (2)$$

dans laquelle apparaît le facteur de massiveté  $\frac{U}{F}$ .

En passant aux différences finies et en explicitant la densité de flux de chaleur  $Q$ , on obtient une équation de résolution permettant de calculer pas à pas la courbe de montée en température du profil [2] [4].

## 2.2. Cas d'un profilé protégé.

Le calcul de la réponse thermique des structures protégées peut être effectué à différents degrés de raffinement.

La méthode la plus simple envisage un bilan thermique restreint ne concernant que l'acier, dans lequel  $U$  est la surface intérieure de l'isolant qui constitue, pour le profilé, la surface émettrice. La massiveté  $\frac{U}{F}$  devient donc dépendante du type de protection.

Dans ce cas, il est nécessaire de faire un certain nombre d'hypothèses concernant la répartition de la température dans l'isolant pour calculer les échanges et les propriétés thermiques moyennes du matériau de protection. On peut alors résoudre l'équation obtenue par itérations comme précédemment.

De telles méthodes ne fournissent des résultats satisfaisants que dans le cas de produits secs et pour des épaisseurs de protection relativement faibles. Pour des problèmes où l'inertie thermique de l'isolant n'est pas négligeable, il faut s'orienter vers des méthodes plus raffinées.

Il existe certaines méthodes intermédiaires, comme celle qui consiste à écrire le bilan thermique de la manière suivante :

$$Q U = c_a \rho_a \frac{\partial \theta_a}{\partial t} F + c_i \rho_i \frac{\partial \theta_i}{\partial t} L_i e_i \quad (3)$$

où  $a$  se rapporte à l'acier et  $i$  à l'isolant.

$L_i$  est la longueur de la fibre moyenne de l'isolant.

Dans ce cas, on peut encore aboutir à une équation en différences finies explicites.



Il faut cependant noter que ces méthodes se heurtent généralement à la méconnaissance des valeurs suffisamment précises de la chaleur spécifique des isolants courants.

### 3. CALCUL AUTOMATIQUE DE LA RESISTANCE AU FEU DE L'OSSATURE.

Pour pouvoir utiliser les théories classiques de l'analyse limite pour le calcul de la résistance au feu du système, il est indispensable de conserver la notion de rotule plastique, donc d'adopter un diagramme contrainte-déformation élastique parfaitement plastique aux différentes températures (figure 3). La limite élastique  $R_e$  décroît alors avec la température suivant une loi connue.

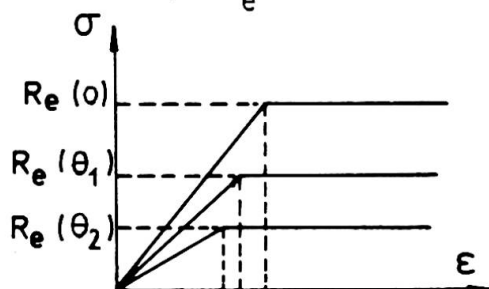


Figure 3

Il s'agit en réalité d'une approximation. Des résultats expérimentaux dus à Magnusson [7] ont en effet montré que le diagramme contrainte-déformation tend à devenir non linéaire aux hautes températures.

Une autre hypothèse concerne la répartition longitudinale de la température dans les profilés.

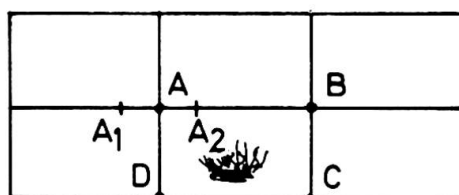


Figure 4

A la figure 4, on a représenté une maille incendiée dans une ossature (ABCD). Dans ce cas, on admet généralement que, pour chacun des éléments AB, BC, CD, DA se trouvant dans la zone incendiée, la température est uniforme d'un bout à l'autre. Aux extrémités A, B, C, D, la température varie brusquement lorsqu'on passe d'une zone incendiée à une zone non incendiée.

Les calculs que nous avons effectués montrent que la distance  $A_1$ ,  $A_2$  sur laquelle se produit le gradient thermique est généralement petite, ce qui justifie l'hypothèse admise.

Pour résoudre ce problème de manière automatique, il existe deux types de méthodes : les méthodes pas à pas et celles utilisant les techniques de la programmation mathématique. Nous avons donné la préférence aux méthodes pas à pas, qui paraissent mieux adaptées ici. En effet, le problème dépend de plusieurs paramètres ; pour le résoudre, il faut le décomposer en une succession de problèmes dépendant d'un seul paramètre.

La solution apportée est une solution du premier ordre, en ce sens que l'on n'a pas tenu compte des effets P.Δ. On a cependant prévu une vérification des colonnes au flambement.

La ruine détectée par le code de calcul correspond à l'apparition d'un des phénomènes suivants :

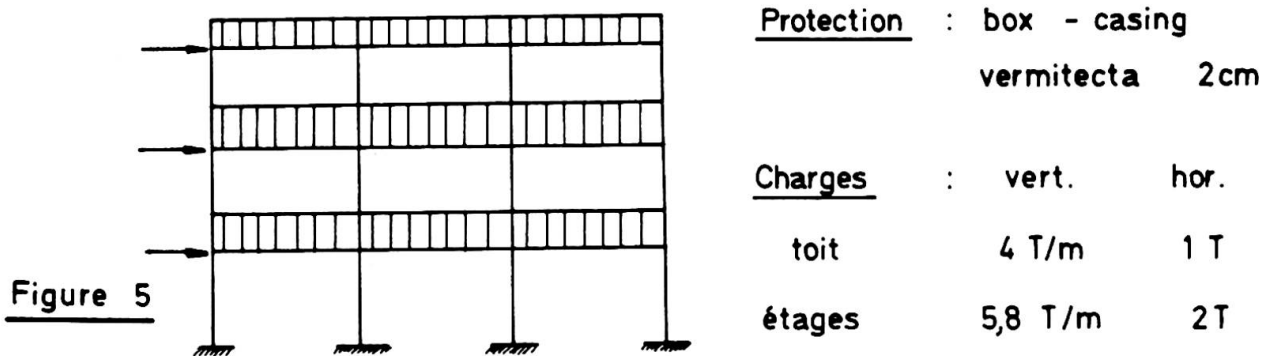
- formation d'un mécanisme d'ensemble ou local (mécanisme de poutre) ;
- instabilité d'une colonne comprimée et fléchie ;
- plastification par effort normal d'un élément massif.



En ce sens, le programme est entièrement automatique : il indique la formation successive des rotules plastiques, l'instant où ces rotules se forment et la durée de résistance au feu, correspondant à la formation d'un des mécanismes de ruine précités.

#### 4. EXEMPLE D'APPLICATION.

Les considérations précédentes sont illustrées par le calcul de la résistance au feu d'un building de 3 étages. Les caractéristiques de l'ossature sont données à la figure 5.



Deux cas différents d'incendies sont examinés. Dans le premier (cfr. figure 6), l'incendie se développe dans la cellule centrale inférieure. La rupture se produit par instabilité de la colonne indiquée après 1 h 23' d'incendie, alors que la température dans l'acier est de 475°. Dans le deuxième cas (cfr. figure 7), un premier foyer se déclare, puis 30 minutes plus tard, l'incendie se propage dans la cellule supérieure. Comme les éléments concernés sont beaucoup moins sollicités, la ruine n'apparaît qu'après 2 h 25', alors que la température dans l'acier est de 730°.

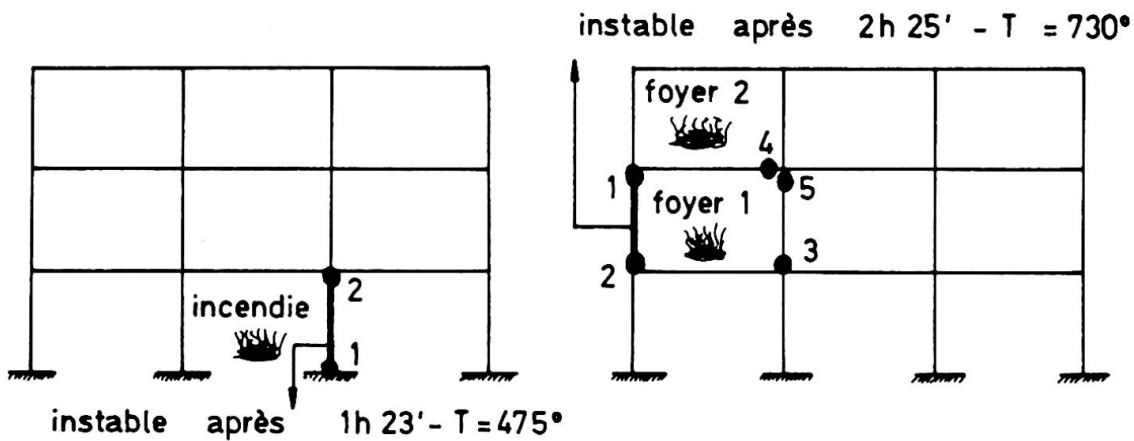


Figure 6

Figure 7

#### 5. CONCLUSIONS.

Cet article fait apparaître l'intérêt des méthodes de simulation pour le calcul de la résistance au feu des structures. L'exemple précédent montre qu'on ne peut pas assimiler la résistance d'un élément essayé isolément à celle qu'il présente dans une ossature complexe. Il met en évidence l'importance de certains facteurs, comme le taux de travail des éléments et la localisation de l'incendie.

## BIBLIOGRAPHIE.

- [1] BEYER, R., KLINGMÜLLER, O., und THIERAUF, G. : Der Feuerwiderstand stählerner Rahmentragwerke. Ansätze zur Berechnung des Brandlastfalles. Rapport Préliminaire, Symposium de l'AIPC sur les Structures en Acier et Mixtes Conçues pour l'Usage, Dresden, 1975, pp.217-223.
- [2] BROZZETTI, J. : Les Principes et les Bases de la Justification par le Calcul du Comportement au Feu des Structures Métalliques. Séminaire UTI-CISCO "La Sécurité de la Construction face à l'Incendie", Saint-Rémy-lès-Chevreuse, Novembre 1975.
- [3] DOTREPPE, J-C. : Modèles Mathématiques pour le Comportement à l'Incendie des Structures. Séminaire UTI-CISCO "La Sécurité de la Construction face à l'Incendie", Saint-Rémy-lès-Chevreuse, Novembre 1975.
- [4] DOTREPPE, J-C.: Préviation par le Calcul du Comportement à l'Incendie des Structures Simples. Rapport de biennale (1973-1975) effectué dans le cadre des recherches de la Commission nationale belge "Recherche-Incendie", Service des Ponts et Charpentes, Liège, Mars 1976.
- [5] DOTREPPE, J-C., et HOGGE, M. : Détermination par la Méthode des Eléments Finis des Evolutions de Température pour les Structures Soumises à l'Incendie. Rapport Préliminaire, 10ème Congrès de l'AIPC, Tokyo, Septembre 1976, pp. 213-218.
- [6] LESCOUARC'H, Y. : Programme de Calcul Elasto-plastique des Structures à Barres par la Méthode Pas-à-pas. Document CTICM 2-09-03.
- [7] PETERSSON, O., MAGNUSSON, S.E., and THOR, J.: Fire Engineering Design of Steel Structures. Manual issued by the Swedish Institute of Steel Construction, Stockholm, 1976.
- [8] SFINTESCO, D. : Calcul et Conception des Structures Métalliques ou Mixtes en vue de leur Résistance à l'Incendie. Rapport Introductif, 10ème Congrès de l'AIPC, Tokyo, Septembre 1976, pp. 125-140.

## RESUME

On présente une méthode théorique pour le calcul automatique de la résistance au feu des ossatures métalliques protégées et non protégées. Le procédé utilisé est apparenté aux méthodes de l'analyse limite des ossatures en acier doux, basées sur le concept de rotule plastique. Un exemple d'application fait apparaître que le choix d'une température critique unique n'est pas réaliste.

**ZUSAMMENFASSUNG**

Man stellt ein theoretisches Verfahren vor, um den Feuerwiderstand geschützter und ungeschützter Stahlbauten automatisch zu berechnen. Dieses Verfahren ist mit dem Traglastverfahren verwandt (plastische Gelenke). Ein Beispiel zeigt, dass die Wahl einer einzigen kritischen Temperatur unrealistisch ist.

**SUMMARY**

A theoretical method is presented for the automatic computation of the fire resistance of protected and unprotected steel structures. The procedure used is rather similar to the method of the limit analysis of steel structures, based on the concept of plastic hinge. An example shows that it is not realistic to adopt only one critical temperature.

### IIIb

#### Justification par le calcul du comportement au feu des structures métalliques

Feuerwiderstandsberechnung von Stahltragwerken

Fire Resistance Calculation of Steel Structures

B. BARTHELEMY

J. BROZZETTI

J. KRUPPA

C.T.I.C.M.

Paris, France

After having done in its research station a great number of fire tests sponsored by the Commission of European Communities (C.E.C.) and the European Conventional Steelwork Associations (C.E.C.M.), the French Technical Center for Steel Construction (C.T.I.C.M.) has developed a method of fire resistance calculation of steel structures.

This calculation requires the knowledge of two different temperatures, which are :

1° The critical temperature of the structure (or only a part of it) which is the steel temperature when the structure can no longer hold its function, i.e. when it collapses either by loss of strength or because of a too large deflection.

2° The steel temperature at the end of the time of stability required by official fire safety rules.

Thus, the knowledge of these two temperatures gives us an answer to the question : will the structure collapse or will it not collapse during the required time of stability ? Or, in other terms : is the critical temperature of the structure higher or lower than the steel temperature at the end of the stability required time ?

Let us explain quickly these calculations :

The critical temperature is mainly dependent upon the loading and type of structure (i.e. statically or non-statically determinate structure) and end restraint conditions. It is not the same for all kinds of structures, as many people believe : it can be 700°C as well as 300°C !

Practically, its determination is made from a flow-chart relating to the temperature the loading rate, i.e. the quotient of the normal loading by the ultimate strength of the structure which is obtained by a plastic calculation. This chart is nothing but the curve giving the decrease with temperature of yield stress of steel (fig. 1).

The calculation is a little bit more complicated when the member is thermally restrained by the rest of the structure which is not affected by fire. In this case, one must calculate the structure rigidity with respect to restraint member in order to determine the supplementary stress induced in the member. Some charts have been drawn to make this calculation easier (fig. 2).

The heating-up behaviour of non-protected steel member is directly read on a chart drawn from a heating formula supposing a heat transfer through the steel uniform and instantaneous (fig. 3). If the member is protected by direct application of fire resistant material such as vermiculite, plaster, etc., the protection is introduced in the calculation by a single coefficient function of temperature which makes the summary of all the thermal properties of the protection in the normal conditions of use of the product. This coefficient is determined by an heating test of protecting members. If there is moisture in the product, the method is slightly different to take into account the water vaporisation level. We have considered that spalling does not occur and that moisture is beneficial for fire endurance.

This method is always simplified by charts giving directly for each product the necessary thickness of protection when the critical temperature and stability time are known (fig. 4).

In summary, this method, though it is justified by complex theoretical calculations, is quite easy to use because many charts have been established. It can be used whatever kind of fire is considered (natural fire or ISO curve), but it cannot yet solve some particular disposals such as external columns, composite structures or members sheltered by suspended ceilings or partition walls. Researches are in progress in France on all these points.

This method of calculation is exposed in detail in a document named "Verification par le calcul du comportement au feu des structures en acier" [1].

#### References

- [1] "Verification par le calcul du comportement au feu des structures en acier"  
Projet de recommandations établies par le CTICM, avril 1976

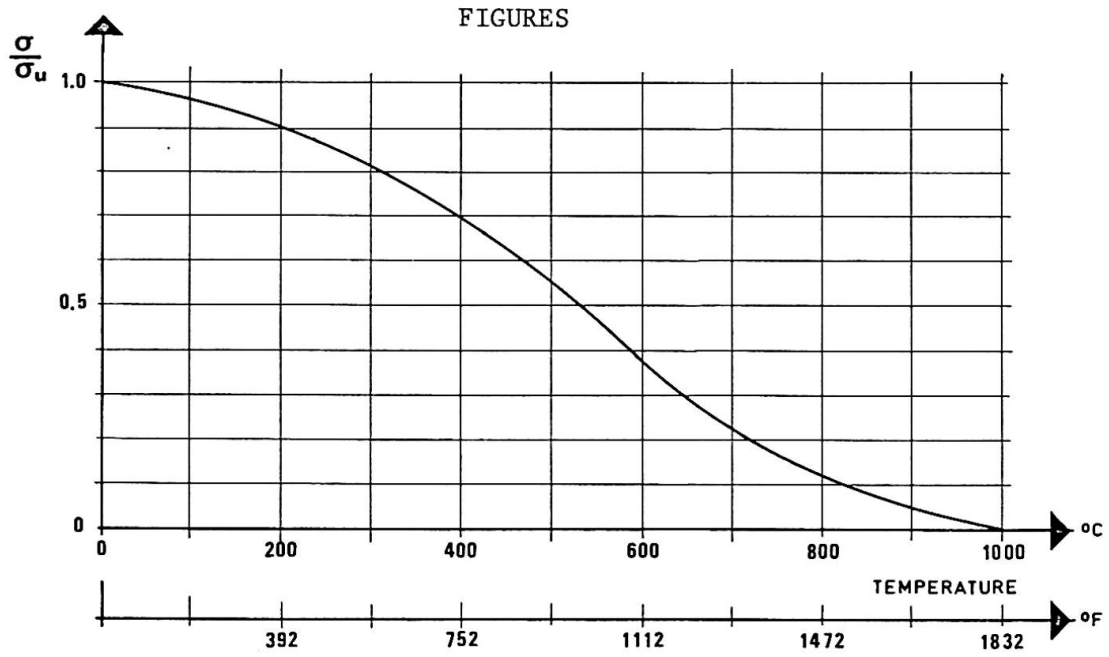


Figure 1 : Chart for calculation of critical temperature.

$\sigma$  : normal loading  
 $\sigma_u$  : ultimate strength

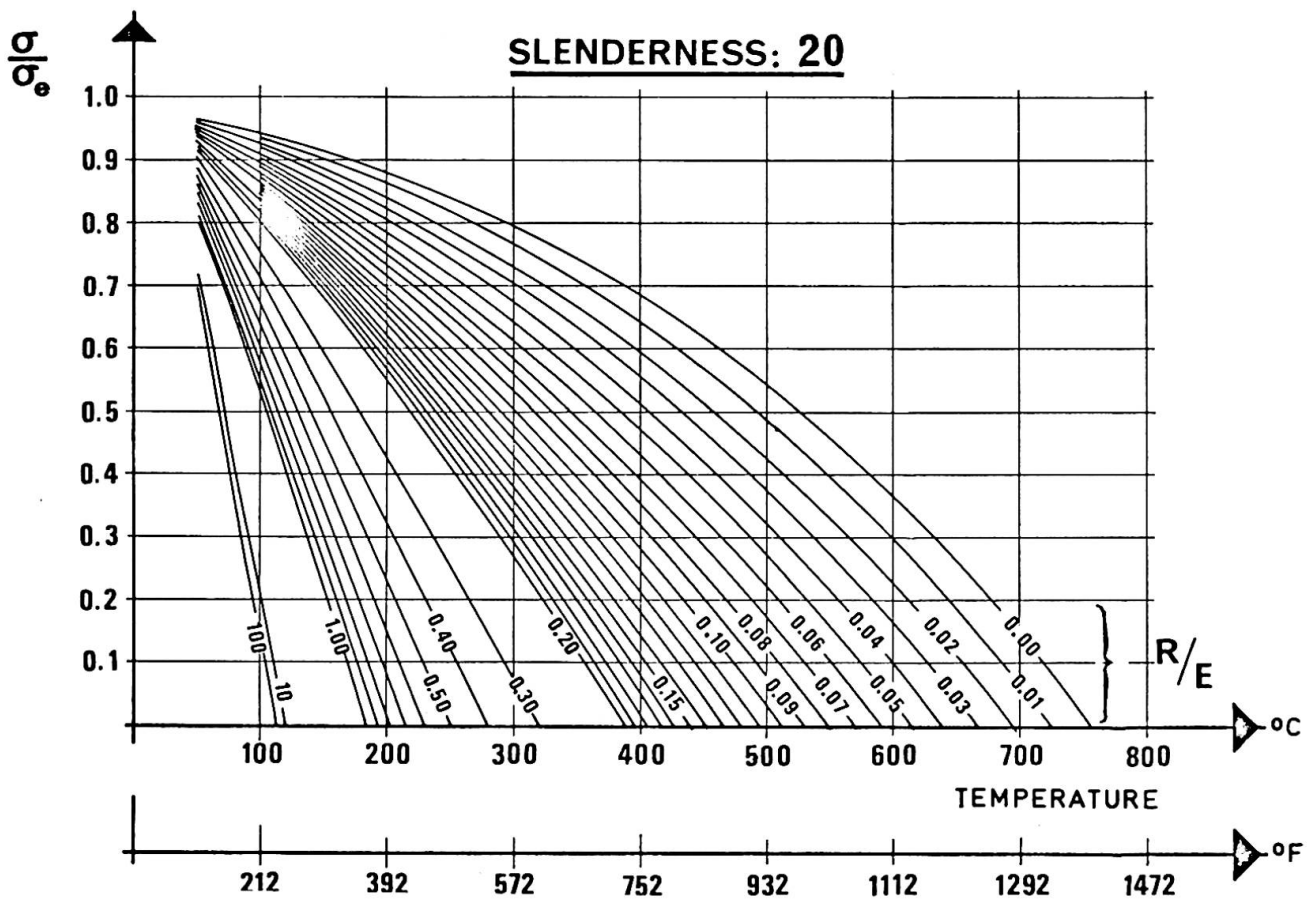


Figure 2 : Example of chart for calculation of critical temperature of a thermally restraint member.

$\sigma_e$  : yield stress  
 $R/E$  : structure rigidity with respect to restraint member

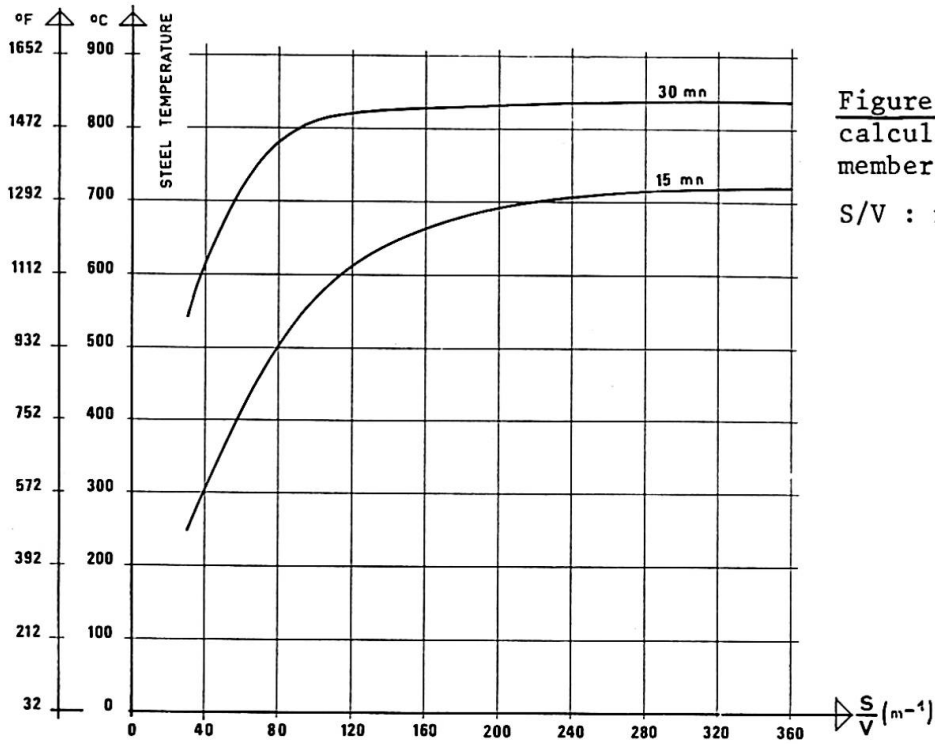
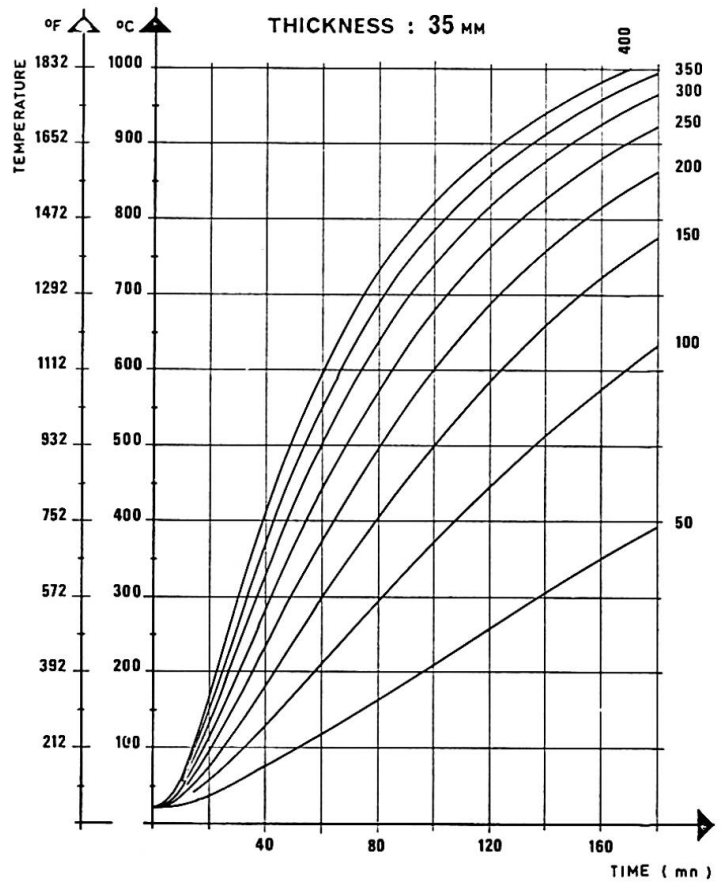


Figure 3 : Chart for heating calculation of non-protected member.

S/V : massivity of member

Figure 4 : Example of chart for calculation of thickness of a given product of protection.



## Theoretical and Experimental Analysis of Steel Structures at Elevated Temperatures

Analyse théorique et expérimentale des constructions métalliques soumises à des températures élevées

Theoretische und experimentelle Untersuchung von Stahlkonstruktionen bei hohen Temperaturen

J. WITTEVEEN      L. TWILT      F.S.K. BIJLAARD  
Professor      Research Engineer      Research Student  
Institute TNO for Building Materials and Building Structures  
Delft, Netherlands

### 1. INTRODUCTION

In principle the reduction in bearing capacity of steel structures under fire action can be determined on the basis of the mechanical properties at elevated temperatures. Some authors [1, 2] solve the problem by using data derived from standard material tests at various temperatures, applying conventional time independent methods of analysis. This procedure has the advantage of being ready for use to designers, but the material tests rather arbitrarily include the creep behaviour, which becomes manifest at temperatures over 400°C. Other authors like Thor [3] and Eggwertz [4] use data derived from conventional creep tests, which are fed into computer programmes, providing the time dependent creep behaviour of structural elements. This method is more reliable but is rather complicated and so far only solutions have been obtained for simple structural elements like beams [3] and columns [4]. Extending this method to more complicated structures like frames encounters practical difficulties. So far, both methods could only be checked by fragmentary experimental data.

In order to arrive at consistent and practical solutions some years ago in the Netherlands work was started combining a theoretical approach with an, in this field, new experimental technique of small scale model tests on beams, columns and frames. For the models, steel bars were used with rectangular cross-sections, with dimensions varying between 5 and 20 mm. The length of the columns and the span of beams varied between 100 and 400 mm. This makes possible a uniform temperature distribution across and along the members, an assumption which also applies to the theoretical analysis. This contribution summarizes the results obtained so far; more detailed information is published in [5, 6].

### 2. DEFORMATION CHARACTERISTICS OF STEEL AT ELEVATED TEMPERATURES

In case of fire in general a structural member will be under constant load and subjected to a temperature increase as a function of time. Depending on the severity of the fire and the insulation of the structural member, the rate of heating can vary. The influence of the rate of heating on the deformation behaviour was studied by analyzing the behaviour of beams and columns on model

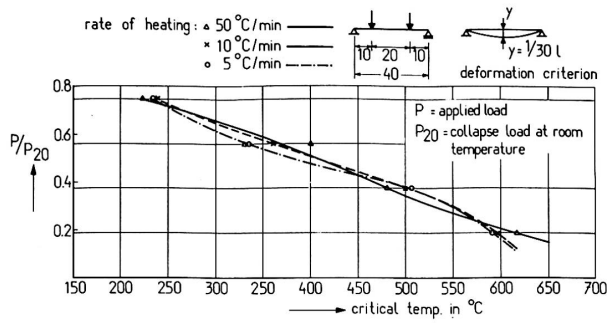


scale, with a constant load and heated with different heating rates. Linear heating rates were chosen of  $50^{\circ}\text{C}$  per minute (approximately corresponding to an unprotected steel member);  $10^{\circ}\text{C}$  per minute (normally protected steel member) and  $5^{\circ}\text{C}$  per minute (heavily protected steel member). In figure 1 the results of beams with a span of 400 mm and a cross-section of  $6 \times 6 \text{ mm}^2$  are summarized. On the vertical axis the applied load is plotted, as a fraction of the collapse load at room temperature, determined experimentally. On the horizontal axis the critical temperature is plotted, being the temperature at which the deflection becomes 1/30th of the span. It follows from the tests that the heating rate does not influence the deformation behaviour in a significant way. For columns similar results were obtained [5]. The results imply that the collapse temperature of steel elements can be considered as time independent, and are consequently not influenced by the heating history. This conclusion makes a theoretical approach possible, which is identical to well known methods at room temperature. Instead of one stress-strain diagram a family of diagrams for different temperatures should than be used. In those stress-strain diagrams creep can be considered as incorporated in the relationships.

To find these relationships non-conventional warm-creep tests were carried out with a loading- and heating procedure similar to the tests on beams described before. A standard cylindrical testpiece was subjected to a constant load and an increasing temperature. In figure 2 a typical result is given. It can be seen that at a certain temperature the elongation increases at constant temperature. This phenomenon is called thermal activated flow. After a certain elongation strainhardening occurs. With Harmathy's theory, slightly modified, the influence of the rate of heating could be determined theoretically. As can be seen the influence of the rate of heating is quite modest. From the warm-creep tests the stress-strain relationships can be derived with a simple transformation. It is emphasised that this transformation is only justified for "practical" heating rates (i.e. between  $5$  and  $50^{\circ}\text{C}$  per minute and temperatures not over, say  $600^{\circ}\text{C}$ ). In addition also stress-strain relationships were obtained by analyzing the small scale beam tests. It appeared that the results obtained by these tests were in reasonable agreement with those obtained by warm-creep tests. In figure 3 a family of stress-strain relationships is presented. The phenomenon of thermal activated flow is visible in this figure by the gap between the relationships applying to  $200^{\circ}\text{C}$  and  $300^{\circ}\text{C}$ . In the subsequent discussion we will consider the family of stress-strain diagrams at elevated temperatures as a starting point for the theoretical analysis of beams, columns and frames.

### 3. RESULTS ON BEAMS

In figure 4 a typical result is given of a simple supported beam loaded with two point loads. As can be seen the results of the calculations are in good agreement with the tests. In this case the complete deformation process as a function of the temperature is given. In practice in many cases only the collapse temperature under a given load is of interest. A much less elaborative procedure can than be used by applying simple plastic theory. In that case only the yield stress at a given temperature derived from the stress-strain relationships has to be used. In figure 5 results are shown of tests on beams with variable end restraints. The beams are framed into columns of which buckling was prevented. By varying the plastic moments of the beams and the columns, the restraint conditions can be varied. It can be seen that the theory is in good agreement with the test results.



temperature at which a maximum midspan deflection is reached as function of the load and the rate of heating (FeE 24)

fig.1

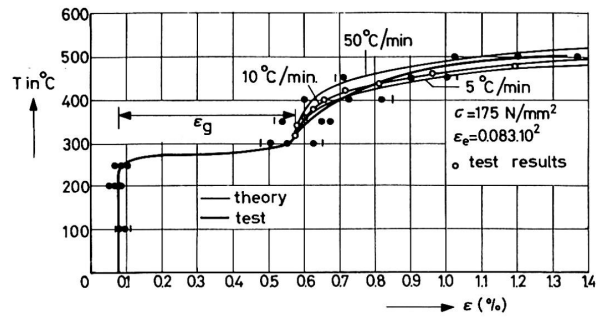
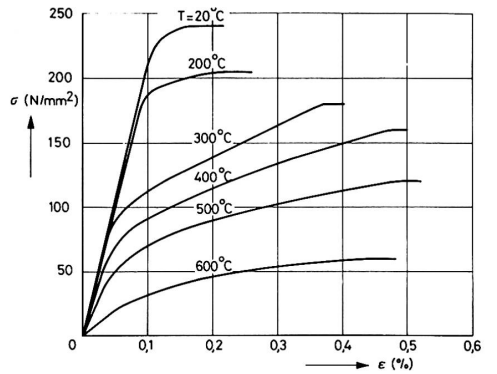


fig.2 T-ε relations for different heating rates



stress-strain relationship of FeE 24 at elevated temperatures

fig.3

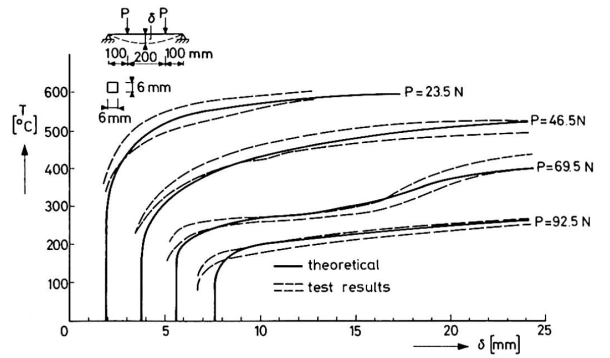


fig.4 temperature-deflection curves of beam at certain load levels.

#### 4. RESULTS ON INDIVIDUAL COLUMNS

In figure 6 computed buckling curves are presented together with experimental results from small scale models. The computations are based on the assumption of an initial out-of straightness of the columns. The value of the out-of straightness is chosen in such a way that at room temperature the computed value of the load bearing capacity coincides with experimental values. In the same figure the buckling curve based on the Dutch design code is given. It is pointed out that the result established for  $600^{\circ}\text{C}$  coincides with a creep buckling analyses by Eggwertz [4] of a column with a slenderness ratio of 45 subjected to a temperature-time history with a maximum of  $600^{\circ}\text{C}$  (allowance is made for difference in yield strength for the respective materials).

#### 5. RESULTS ON BRACED AND UNBRACED FRAMES

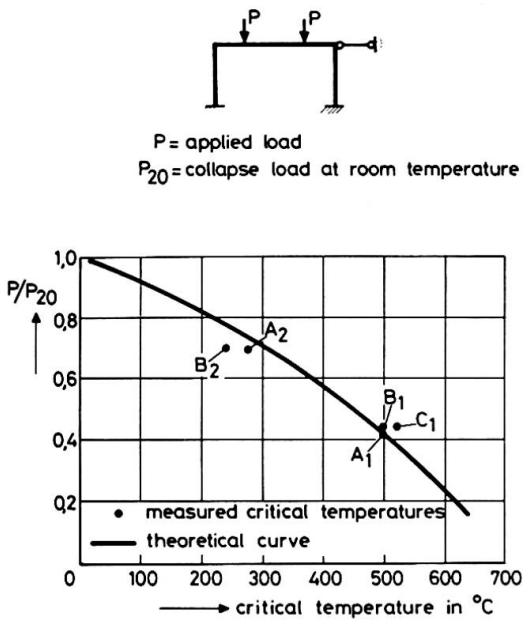
The analysis can take place in the same way as applicable to structures at room temperature, and needs no extensive discussion. As can be seen from figure 3 the deformation behaviour is non-linear, and as a consequence for the structural analysis, computer techniques must be used. Recently, however, computer programmes are available in which physical non-linearity as well as geometrical non-linearity can be taken into account. In connection with physical non-linearity there is one complication to be discussed here. The unloading characteristics of steel at elevated temperatures are not well established yet. For the time being, an elastic unloading behaviour is assumed, of which the path of unloading coincides with the path of loading. This assumption in general leads to lower bound solutions.

In figure 7 the results of theoretical and experimental analyses are summarized for braced frames. By variation of the cross-sectional dimensions two types of frames were obtained with different effective slenderness ratio's. Two different load levels  $P$  were applied, defined as a fraction of the collapse load  $P_{20}$  at room temperature. In addition loads  $K$  have been applied, chosen in such a way that the linear elastic moment at the top of the column equals one half of the moment producing the yield stress in the outmost fibres of the column. It follows from figure 7 that the theoretical predicted collapse temperatures are slightly lower than those resulting from the experiments. This trend is not surprising considering the simplifying assumption of elastic unloading characteristics of steel at elevated temperatures.

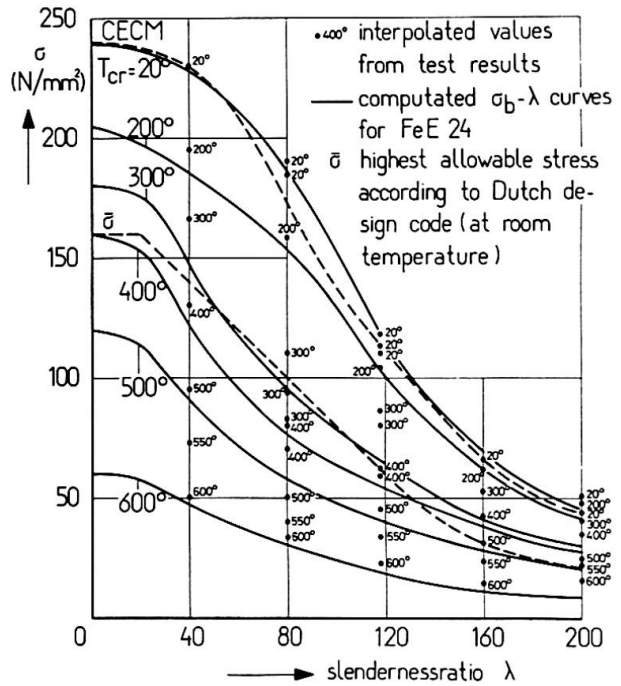
Analyzing the stability of unbraced frames it becomes apparent that the initial inclination of the frame under vertical load is an important factor. This is illustrated in figure 8 where a typical result is given of an unbraced frame with the same loading type as for the braced frames. It follows that the theoretically derived collapse temperature is substantially influenced by the mode and magnitude of the inclination. As can be expected maximum values are found if the mode of inclination is symmetric. It can be seen that the test results are conservative compared with the theoretical values. In [6] results are described of unbraced frames with additional horizontal loads.

#### 6. CONCLUSIONS

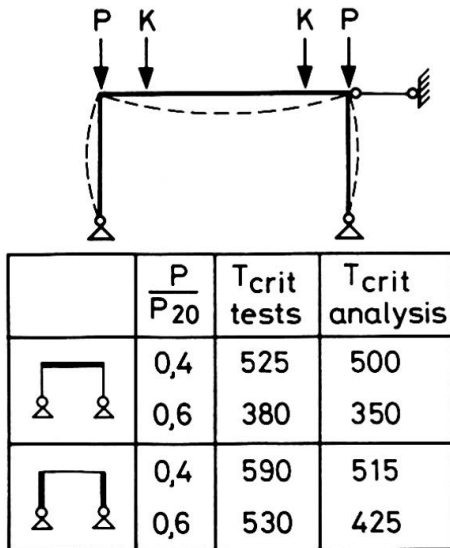
Summarizing it can be stated that the presented method, describing the behaviour of beams, columns and frames at elevated temperatures seems reliable. A basic feature is that the deformation characteristics of steel at elevated temperatures can be considered as time independent. Further activities are going on to implement the method for real structures and make it ready for use



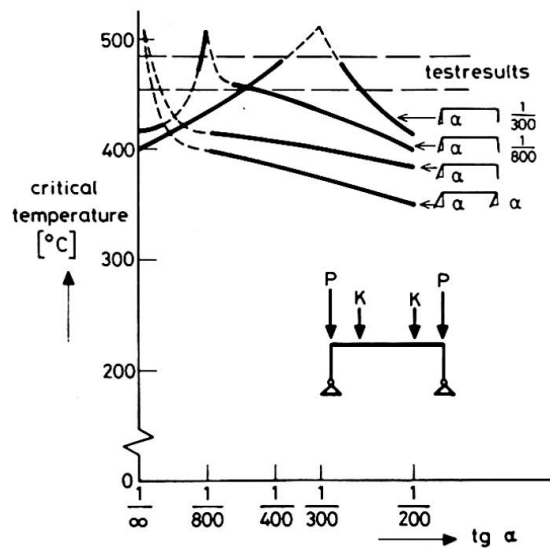
comparison between calculated and measured critical temperatures of beams with different end restraint (instability prevented)  
 fig.5



relationship between critical stress and slenderness-ratio at different temperatures  
 fig.6



theoretical and test results of braced frames  
 fig.7



relationship between the inclination  $\alpha$  and the critical temperature of an unbraced frame at elevated temperatures ( $P = 0,6 P_{20}$ )

fig.8

to designers. The assumption of a uniform temperature distribution along and across the members is not essential. An extension to non-uniform heating can easily be realized.

#### REFERENCES

1. Kawagoe, K. and H. Saito, "Thermal effects of fire in buildings", IABSE 10th Congress, Introductory Report, Zürich 1976.
2. Sfintesco, D., "Calcul et conception des structures métalliques ou mixtes en vue de leur résistance a l'incendie", IABSE 10th Congress, Introductory Report, Zürich 1975.
3. Thor, J., "Deformations and critical loads of steel beams under fire exposure conditions", National Swedish Building Research Document, 1973.
4. Eggwertz, S., "Creep buckling of steel columns at elevated temperatures", IABSE 10th Congress, Preliminary Report, Zürich 1976.
5. Witteveen, J. and L. Twilt, "Behaviour of steel columns under fire action", International Colloquium on Column Strength, Proceedings IABSE, Volume 23, Zürich 1975.
6. Witteveen, J. and L. Twilt, "The stability of braced and unbraced steel frames at elevated temperatures", Second International Colloquium on Stability of Steel Structures, Preliminary Report, 1977.

#### SUMMARY

In this study the deformation characteristics of steel at elevated temperatures are derived from creep tests as well as from small scale model tests on beams. As a result the load bearing capacity of steel structures under fire action can be determined with the well known methods used at room temperature. Both theoretical and experimental results of beams, columns and frames are summarized.

#### RESUME

Dans cette étude les caractéristiques de déformation de l'acier aux températures élevées sont déterminées par des essais de fluage et par des essais à échelle réduite sur des poutres. La résistance des constructions métalliques au feu peut ainsi être déterminée à l'aide des méthodes bien connues, utilisées aux températures ordinaires. Les résultats théoriques et expérimentaux sont présentés pour des poutres, poteaux et cadres.

#### ZUSAMMENFASSUNG

In dieser Untersuchung sind die Verformungseigenschaften von Stahl bei hohen Temperaturen aus Kriechversuchen und aus Modellversuchen in kleinem Massstab an Trägern ermittelt. Die Tragkraftfähigkeit von Stahlkonstruktionen unter einer Brandbeanspruchung kann mit den bekannten Verfahren bei normalen Temperaturen ermittelt werden. Theoretische und experimentelle Resultate für Träger, Stützen und Rahmen sind zusammengefasst.

**Creep Buckling of a Steel Column in a Temperature-Time History Simulating a Fire**

Flambage par fluage d'un poteau en acier selon un diagramme température-temps simulant un incendie

Kriechknicken von Stahlstützen in einem Temperatur-Zeit Verlauf, der einen Brandfall simuliert

SIGGE EGGWERTZ  
The Aeronautical Research Institute  
Stockholm, Sweden

1. INTRODUCTION

At temperatures exceeding 500°C ordinary carbon steels show a high creep rate even at low tensile or compressive stresses. In a paper published in the Preliminary Report of the 10th Congress of IABSE [1] the author presented results of creep buckling calculations for a steel column of section HE 240B with a yield strength of 300 MPa. A computer programme prepared at the Aeronautical Research Institute of Sweden [2] was used to obtain the creep buckling life of columns of various lengths subjected to a number of different mean compression stresses assuming a constant temperature of 600°C. A diagram was given where the buckling stress was plotted versus the slenderness ratio  $\lambda$  for times of exposure to this temperature ranging from 0.2 to 2.0 h. The diagram showed quite clearly that time is an important parameter which must be considered when analysing the buckling strength of a steel column at elevated temperatures.

The temperature during a fire varies, however, with a rise from room temperature to a maximum, determined by the fire load, after which the cooling starts, usually at a much lower rate than the heating. The computer programme mentioned was therefore modified to allow variations in temperature. A few calculations with such temperature histories assuming maximum temperatures 600°C and 650°C respectively were carried out and presented already in Ref [1]. This investigation has been continued. By repeated life calculations, the compression stress was determined which just resulted in creep buckling collapse at the end of a temperature-time history with a maximum of 600°C. This was done for the slenderness ratios  $\lambda = 30, 45, 60$  and  $90$ .

## 2. CALCULATIONS

The modified version of the creep buckling computer programme is able to take into account a linear increase in temperature from an initial value to a maximum  $\vartheta_{\text{max}}$ , then a constant period and finally a linear decrease in temperature. The creep law of Norton-Odqvist is utilized

$$\dot{\epsilon} = k\sigma^n$$

where the exponent  $n = 4.9$  is assumed to be constant for all temperatures considered, while the creep coefficient  $k$  varies with the temperature  $T$  K

$$k = 1.88 \times 10^{-11} \exp(44.7 - 39000/T)$$

Young's modulus, including elastic and plastic deformation, as well as primary creep, is determined by the relation

$$E_0 = 325000 - 404 \vartheta_s \text{ MPa}$$

The numerical calculations were performed for a temperature-time history shown in Fig 1 with heating and cooling rates  $1000^\circ\text{C/h}$  and  $333^\circ\text{C/h}$  respectively, and further  $\vartheta_{\text{max}} = 600^\circ\text{C}$  lasting for a period of 0.2 h. The radius of gyration in the buckling direction of the chosen column section HE 240B is  $i = 0.10$  m. The assumed lengths were 3.0, 4.5, 6.0 and 9.0 m.

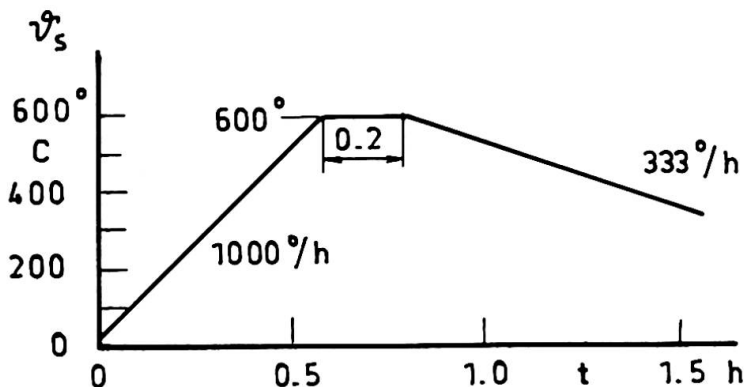


Fig 1 Temperature-time history introduced into computer programme

## 3. RESULTS AND DISCUSSION

After a number of trials with different loads on the column section it was found that for the slenderness ratios  $\lambda = 30, 45, 60$  and  $90$  the mean stresses  $\sigma = 60, 51, 41$  and  $28$  MPa respectively would result in creep collapse just at the moment of the temperature-time history during the cooling phase where creep had practically ceased. The results have been plotted in Fig 2 together with the creep buckling curves obtained earlier [1] for constant temperature exposure times. It was discovered that the value determined before with  $\lambda = 45$ , for a history with the maximum temperature  $600^\circ\text{C}$ , was somewhat too high due to an unconservative interpolation. The temperature-time history of Fig 1 seems to have about the same effect as if the column had been exposed to a constant temperature of  $600^\circ\text{C}$  during 0.5 h. This result is not surprising since the temperature in Fig 1 exceeds  $500^\circ\text{C}$ , where the rapid creep starts, during 0.6 h. Further investigations are likely to show the feasibility



of using constant temperature buckling curves to determine the critical stress of a column subjected to a fire temperature history.

The buckling analysis presented in Fig 2, although considering a realistic fire history of the mean temperature of the steel column, still neglects other complications met in practice such as temperature gradients and residual stresses within the column, as well as restraining forces from other structural elements. Thus, it is not claimed that Fig 2 may be used directly for design purposes. It seems to represent a substantial improvement, however, in comparison with the two dotted curves given by the general reporters, Theme III, in the Introductory Report of the Congress [3]. The analysis clearly shows that creep has to be taken into account at fire temperatures exceeding 500°C, where time is consequently an important parameter. This conclusion was supported in the Prepared Discussion contribution by Fukumura [4].

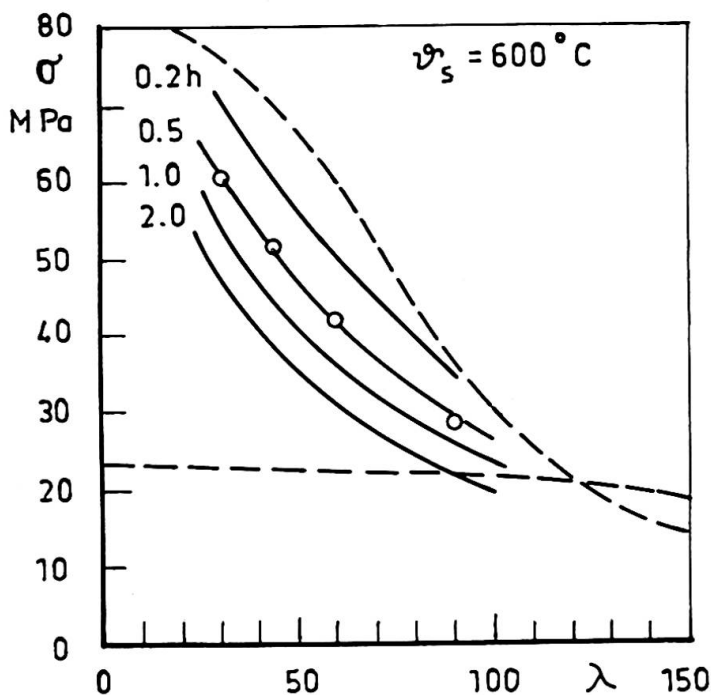


Fig 2 Buckling stress versus slenderness ratio for various times of exposure to 600°C and for temperature-time history with maximum temperature 600°C

#### REFERENCES

1. Eggwertz, S: Creep buckling of steel column at elevated temperatures. IABSE 10th Congress, Preliminary Report, Zürich 1976, p 235-240
2. Samuelson, Å: Creep deformation and buckling of column with an arbitrary cross section. FFA Report 107, Stockholm 1967
3. IABSE 10th Congress, Introductory Report, Zürich 1975, p 117 and 135
4. Fukumura, F: Inelastic behavior of protected steel column in fire. IABSE 10th Congress, Prepared Discussion, to be published in the Final Report, 1977



## SUMMARY

The creep buckling stress was determined by computer analysis for steel columns subjected to a realistic fire temperature history with a maximum of 600 °C. The results were compared to earlier calculations with constant temperature of 600 °C. The influence of creep was still found to be important.

## RESUME

La contrainte de flambage par fluage de poteaux en acier a été déterminée par des calculs numériques selon un diagramme température-temps simulant un incendie avec un maximum de 600 °C. Les résultats sont comparés aux calculs déjà faits pour une température constante de 600 °C. On constate que l'influence du fluage reste importante.

## ZUSAMMENFASSUNG

Die Kriechknickspannung wurde für Stahlstützen durch ein numerisches Programm für einen Temperatur-Zeit Verlauf mit maximum 600 °C bestimmt, der einen Brandfall simuliert. Das Resultat wird mit früheren Berechnungen mit einer konstanten Temperatur von 600 °C verglichen. Der Einfluss des Kriechens ist von Bedeutung.

**Inelastic Behaviour of Protected Steel Columns in Fire**

Comportement inélastique des poteaux protégés contre l'incendie

Nichtelastisches Verhalten von feuergeschützten Stahlstützen

F. FURUMURA                      Y. SHINOHARA  
Associate Professor                  Graduate Student  
Tokyo Institute of Technology  
Tokyo, Japan

**1. Introduction**

The fire resistance of structural members has been determined in the past by subjecting isolated members to standard fire tests. More recently, calculations based on heat transfer and the structural properties of materials at high temperature have been used to replace the costly and time-consuming standard fire tests. In the past the cost of testing precluded considerations of assuming more realistic situations corresponding to columns in continuous structures subjected to fires representing actual conditions. These more realistic situations can now be studied by computer calculation.

In this work three aspects for protected steel columns are studied: (1) the stress distribution in a column during fire, (2) the interaction of an interior column exposed to fire with the surrounding building structures, and (3) the fire resistance of columns which take into account creep deformation behavior.

This work is a continuation of Ref.1 and the method of analysis regarding determination of stress, strain and deformation of the column are contained therein.

**2. Calculation of Temperature Rise**

A computer program was written to calculate the temperatures within a column when the temperature outside four faces was raised in the manner specified for fire tests in JIS A 1304.

Most columns used in buildings have sections less than 15 cm thick. In such cases detailed calculation of temperature distribution in the steel cross section is unnecessary, and one-dimensional model of the heated column can be usefully employed.<sup>(2)</sup> The model consists of a steel plate having the same cross-sectional and surface areas per unit height as the four sides of the heated column, with the edges and unexposed side perfectly insulated. This model permits use of a one-dimensional numerical procedure.

In calculating the temperatures, furthermore, it was assumed that fire protection panels became divided into a dry zone and a wet zone, within each of which the thermal properties were taken to be constant.

It was also assumed that vaporization occurred at atmospheric pressure at the interface between these zones, and that therefore interface moved away from the heated face as drying penetrated into the protection. Typical results, for the temperatures in H cross-section steel columns with 3 or 5 cm thick protection, are shown in Figures 1 and 2.

### 3. Stresses and Strains in a Column during Fire

To analyse the strain and stress in a column section, the following assumptions were made:

(1) Plane sections remain plane. This assumption is approximately correct for long prismatic members in continuous construction.

(2) The free expansion of steel due to temperature change,  $\epsilon_T$ , is assumed as follows ( see Fig.3 ) :

$$\epsilon_T = 5.04 \times 10^{-4} T^2 + 1.13 \times 10^{-5} T \dots\dots\dots (1)$$

where T is in degrees Centigrade.

(3) The relationship between steel stress  $\sigma$ , and strain  $\epsilon$ , in compression, is assumed as follows (see Fig.4) :

$$\epsilon E_o(T) = C(T)\sigma - [1 - C(T)]\sigma_y(T) \ln[1 - \sigma/\sigma_y(T)] \dots\dots\dots (2)$$

where

$$E_o(T) = 2.15 \times 10^6 [0.745 + 0.137 \ln[-0.01T + 6.3]] \quad (\text{kg/cm}^2)$$

$$\sigma_y(T) = 5.0 \times 10^3 [-4.49 \times 10^{-9} T^3 + 3.57 \times 10^{-6} T^2 - 1.41 \times 10^{-3} T + 1.027] \quad (\text{kg/cm}^2)$$

$$C(T) = -4.0 \times 10^{-4} T + 1.0$$

In this expression  $\sigma_y(T)$  is the steel yield point (SM 58),  $E_o(T)$  is the initial tangent modulus and  $C(T)$  is a parameter that affects the form of the stress-strain curve as shown in Figure 4, in which T is expressed in degrees Centigrade. Besides these data, the material description must include behavior during unloading and in tension. This is arranged by making the following two assumptions: (1) Behavior in tension is the same as that in compression, and (2) Behavior during unloading from ( or reloading to ) a previously obtained value of a compressive stress given by equation 2 is linear  $d\sigma/d\epsilon = E_o(T)$ , the initial tangent modulus.

(4) To evaluate the creep deformation, it is assumed that the creep strain for SM 58 is related to time t, absolute temperature  $T'$ , and current stress  $\sigma$  in the form such that, ( see Fig.5 )

$$\epsilon_c = [10^{c-a/2.3T'}] X [ [2.37\sigma/5.0]^{b/2.3T'+\alpha} ] t^n/n \dots\dots (3)$$

where  $c=20.53$   $b=1.9 \times 10^4$   $\alpha=-7.25$   $n=0.35$   $a=4.5 \times 10^4$

t: minutes  $\sigma$ : kg/mm<sup>2</sup>  $\epsilon_c$ : %

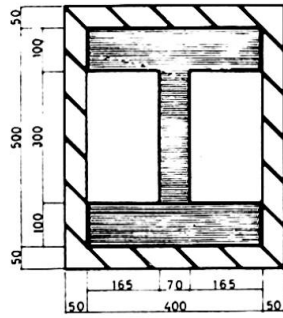
The strain-hardening creep law is applied for the calculation of the nonstationary creep deformation.

(5) The column is divided into blocks with 1/20 or 1/40 column length in the axial direction and each block is subdivided further into 20 elements in the cross sectional direction. For each element the strain, stress and material properties are assumed uniform.

(6) Initial stresses and strains in the cross-section before the fire, are determined, assuming that the axis of the column has initially the form of a sine curve which takes into account the various imperfections in a column.

(7) It is assumed that there are no cases in which a steel column subjected to compression will buckle torsionally or locally and the effect of shearing force on the deformation can be neglected. Buckling of the column will occur in the plane of minimum flexural rigidity.

Figure 1 SECTION



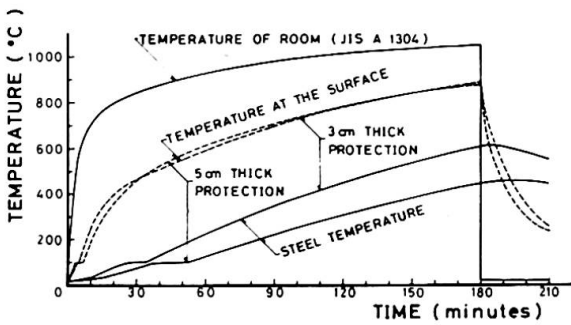
STEEL COLUMN  
(SM58)

Young's modulus	$2.15 \times 10^4$ Kg/cm <sup>2</sup>
Strain corresponding to the yield stress	$2.50 \times 10^{-4}$ %
Yield stress	$5.00 \times 10^3$ Kg/cm <sup>2</sup> (20°C)

FIRE PROTECTION  
(CONCRETE)

Thickness	3.0 or 5.0 cm
Percentage of moisture content	4.0 %
Specific gravity	2340 Kg/m <sup>3</sup>

Figure 2 CALCULATED TEMPERATURE OF PROTECTED STEEL



FREE THERMAL STRAIN-TEMPERATURE CURVE

Figure 3

$$\epsilon_T = 5.04 \cdot 10^{-9} \theta^2 + 1.13 \cdot 10^{-5} \theta$$

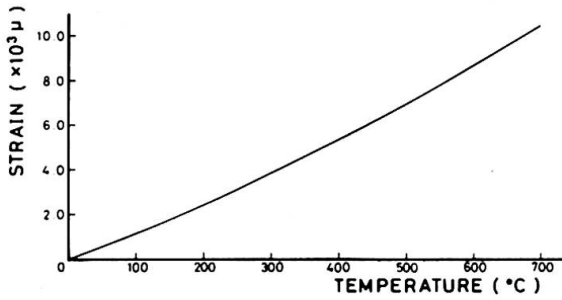


Figure 4 ASSUMED STRESS-STRAIN CURVE (based on Harada and Furumura's Data)

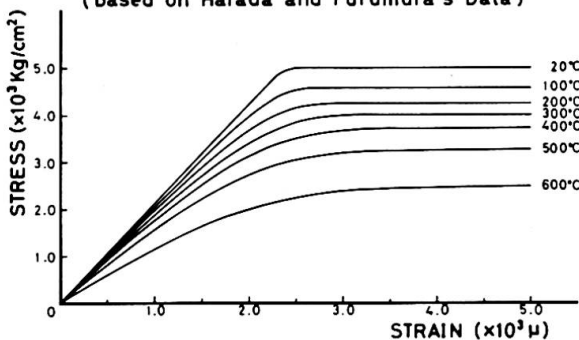
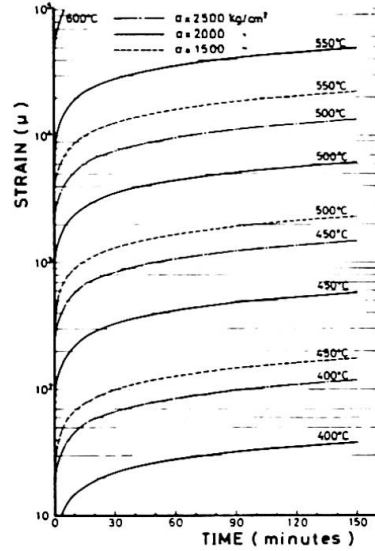
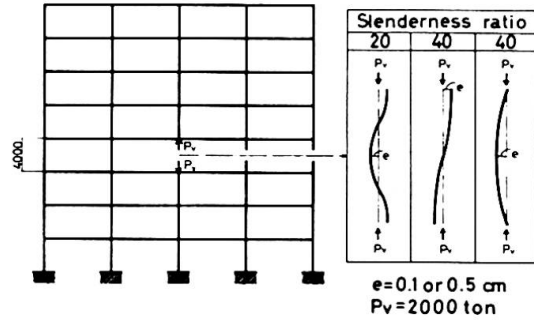


Figure 5 NONSTATIONARY CREEP

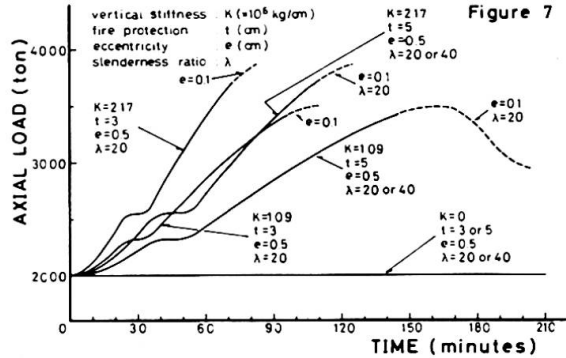


STRUCTURAL ARRANGEMENT OF BUILDING FRAME AND HEATED COLUMN

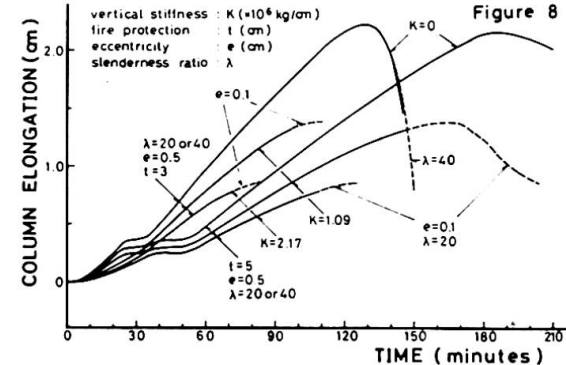
Figure 6



COLUMN-STRUCTURE INTERACTION DURING FIRE



COLUMN-STRUCTURE INTERACTION DURING FIRE



Based on these assumptions, the distribution of strain and stress is calculated for each 5-minute interval during fire. The method of analysis is to determine, by trial and error, a linear strain distribution in the steel which provides equilibrium of the cross-section.

#### 4. Interaction of a Single Column and Surrounding Structure

A column expands during a fire and, because of the resistance of the surrounding structure to this expansion, more than the initial dead plus live load is attracted to the column.

If every column in a floor were subjected to the same fire, all the columns would expand equally and additional load would not be attracted to any one column. If only one of the floor columns were exposed to fire, the expansion of the column would be resisted by the surrounding structure. The greater the number of slabs above the column, the greater the resistance, and the greater the load attracted to the column.

The correct solution to the interaction problem requires a trial and error determination of moments, curvatures and displacements along the column for each point in time.

#### 5. Results of Calculation

It is clear that a combination of axial load and axial and flexural restraint would arise with the structural arrangement shown in Figure 6.

To calculate lateral deflection, two cases of the flexural restraint for H cross-section steel column are assumed: (1) The column has both ends built in, and (2) The column is built in at the lower end and is free to displace laterally at the upper end but is guided in such a manner that the tangent to the deflection curve remains vertical, and that is equivalent to the case of a column with hinged ends.

The former assumption is considerably in error early in a fire during elastic conditions, but appears to be approximately correct as the column approaches failure when it bends with large inelastic strains at the critical sections. The latter is considered to be corresponded to the case in which every column in a floor would be subjected to the same fire.

Figure 7 shows how the applied load (initial load = 2000 ton/a column) increases by the interaction effect. Figures 8 and 9 to 11 show the corresponding column lengthening and lateral deflection, respectively.

The interaction effect is shown clearly in Fig. 7. The curve labelled "K=0", which corresponds to the assumption of no interaction, serves as a basis for comparison. As the vertical stiffness of the surrounding structure increases from 0 to  $1.09 \times 10^6$  kg/cm, which corresponds to 1/5 vertical stiffness of a column with 4 m length, the applied load more increases and the fire resistance is decreased, as seen by comparing column movements. As the vertical stiffness is increased further to  $2.17 \times 10^6$  kg/cm, the fire resistance is more decreased. The fire resistance is also effected by the protection thickness.

Figures 12 to 14 show the variations of the strain, stress and tangential modulus in the extreme element on the convex side of the critical section. Figure 15 and 16 show the variations of the curvature distribution of the columns.

From the numerical results, the column is not greatly affected by creep until the steel temperature reaches  $450^\circ\text{C}$ . After  $450^\circ\text{C}$ ,

COLUMN-STRUCTURE INTERACTION DURING FIRE

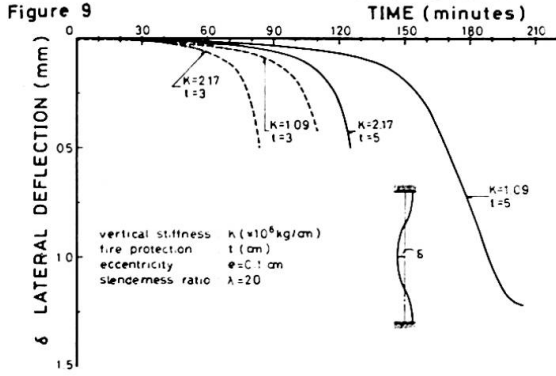
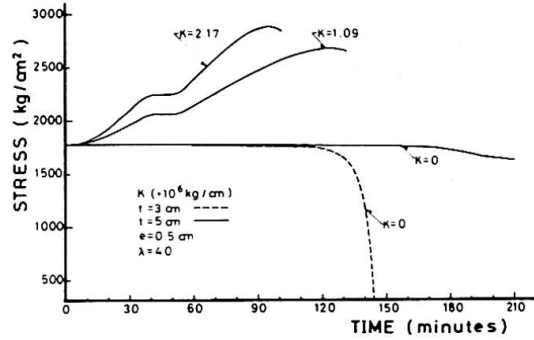


Figure 13 STRESS-TIME CURVES DURING FIRE ELEMENT (1,20)



COLUMN-STRUCTURE INTERACTION DURING FIRE

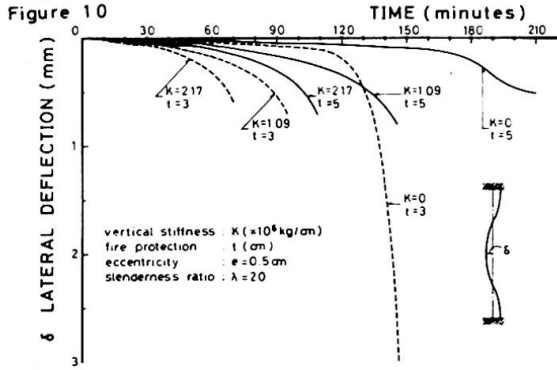
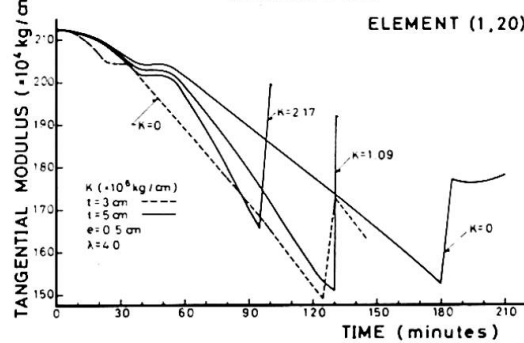
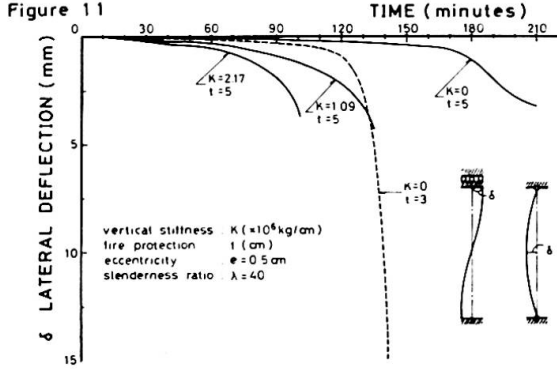


Figure 14 TANGENTIAL MODULUS-TIME CURVES DURING FIRE ELEMENT (1,20)



COLUMN-STRUCTURE INTERACTION DURING FIRE



CURVATURE DIAGRAMS due to BENDING MOMENT

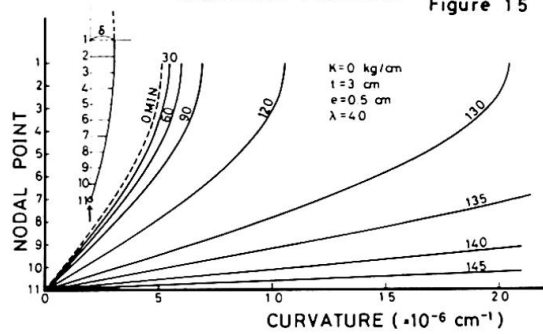
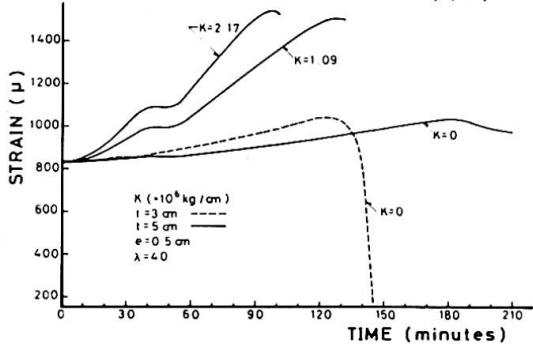
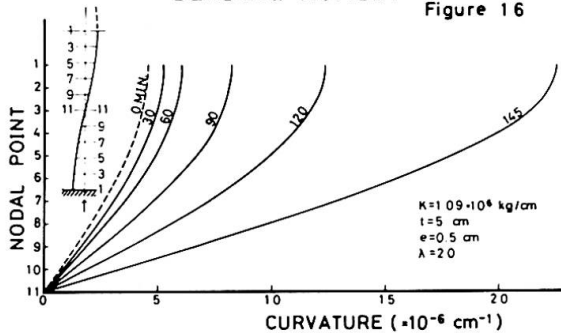


Figure 12 STRAIN-TIME CURVES DURING FIRE (due to stress) ELEMENT (1,20)



CURVATURE DIAGRAMS due to BENDING MOMENT





the creep rate increases rapidly and the column causes chord shortening, followed by lateral bending and relief of the applied load.

For very stiff vertical resistance the column buckles quite early, and the greater the initial deflection, the earlier the buckling of the column.

## 6. Conclusions

This study represents an initial attempt to evaluate in detail the behavior of a steel frame structure in a fire.

The creep deformation of columns in transient heating processes is of considerable interest to engineers working in the field of fire protection.

A numerical technique has been described in Ref.(1). The technique utilized a creep model was originally suggested by England<sup>(3)</sup> and Dougill<sup>(4)</sup> and expanded by the authors to suit certain practical requirements. The calculations that have been undertaken have been based on an idealized model of material behavior and it is doubtful whether the numerical values obtained have any significance in themselves. However, some aspects being important to understand modes of behavior of columns in fire have been found out and the information obtained from such detailed analysis is very useful in the future development of a simple and rational procedure for fire safety design of high rise steel structures.

## 7. References

- (1) Furumura, F., and Konishi, T., "Inelastic Behavior of Reinforced Concrete Wall Exposed to High Temperatures", Report of the Research Laboratory of Engineering Materials, No.1, Tokyo, 1976, pp.31-47.
- (2) Stanzak, W.W., and Lie, T.T.; ASCE, Journal of the Structural Division, May.1973, pp.837-852.
- (3) England, G.L., and Ross, A.D.; Magazine of Concrete Research, V.14, No.40, Mar.1962, pp.5-12.
- (4) Dougill, J.W.; Magazine of Concrete Research, V.24, No.80, Sep. 1972, pp.139-148.

## SUMMARY

The study shows the inelastic behaviour of protected steel columns under fire action. It is shown that the effect of creep on the buckling strength is very important at temperatures more than 450° C.

## RESUME

L'étude s'occupe du comportement inélastique des poteaux métalliques protégés contre l'incendie. Il est montré que l'influence du fluage est très importante pour les températures supérieures à 450° C.

## ZUSAMMENFASSUNG

Das nichtelastische Verhalten von geschützten Stahlstützen bei Brandbeanspruchung wird untersucht. Es wird gezeigt, dass dem Kriechen bei Temperaturen über 450° C grosse Bedeutung zukommt.



**Design of Fire- and Impact-Resistant Ceilings in a Medieval Castle**

Conception de plafonds résistant aux chocs et à l'incendie, dans un château médiéval

Entwurf von stoss- und brandsicheren Decken in einem mittelalterlichen Schloss

**JIRI HEJNIC**Chief Engineer, Bridge Department  
Institute for Traffic and Structural Engineering Design  
Prague, Czechoslovakia**1. Introduction**

Karlštejn Castle is a quite exceptional example not only among Czech castles but in the whole of Middle Europe at all. It was built in the 14th century by Charles IVth, Czech king and since the year 1346 the Emperor of the Roman - German Empire, one of the greatest rulers of his time. The Castle /Fig. 1/ was erected to be not only a place of private retreat for the monarch, but also a noble shrine for a large collection of relics of saints which was enlarged in the year 1350 with crown - jewels of the Roman - German Empire. The most costly part of the treasure was, however, the crown of Charles the Great, a symbol of sovereign power over the whole Middle Europe.

**Fig. 1 Karlštejn Castle**

Important parts of the Castle are the Emperor's residence adjoined directly with the neighbouring Chapel of Virgin Mary by means of a wooden passage.

This church in the second floor of the tower - building was covered with an ornamental beam - ceiling. On three walls mural paintings from the Apokalypse are preserved together with three other scenes concerning directly important events leading to the foundation of the Castle. They are of extraordinary importance in the Gothic painting being ones of the first realistic portraits, especially those of Charles IVth. The Church of Virgin Mary had a direct connection with a donjon, which was the most solid and most important building of the whole Castle. The central room of this donjon and at the same time of the whole Castle is the Chapel of the Holy Cross on the second floor, characterised by Gothic windows, glassed partly with finely cut semiprecious stones. In a special niche behind the altar a treasure of greatest importance for the State - the crown jewels of the Roman - German Empire - was hidden. However, the greatest treasure for us now is a large medieval set of 128 Gothic tablets, representing saints and saintesses in half - figures in rare completeness /Fig. 2/.

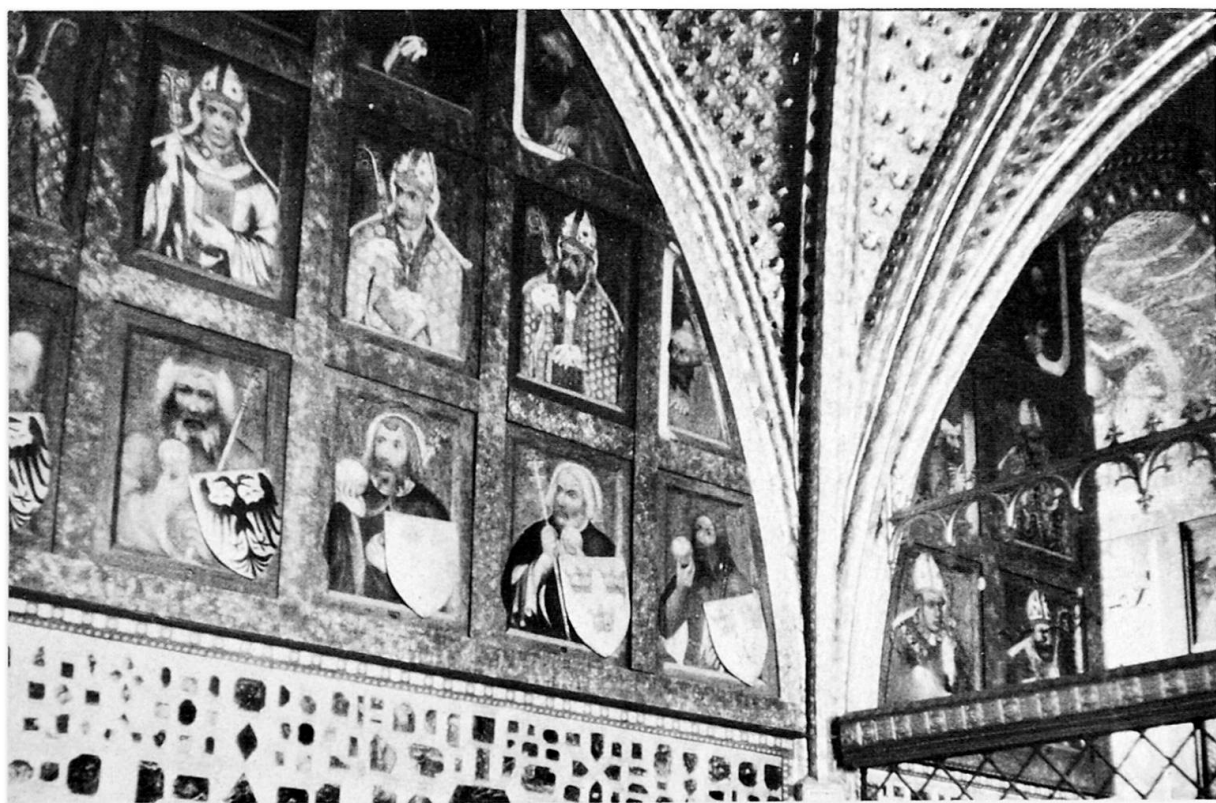


Fig. 2 Interior of the Chapel of the Holy Cross

The restoration of the Castle, carried out in the years 1888 - 1904 removed almost all traces of later renovations, made toward the end of the 16th century. The ancient and venerable Castle, the real memorial of Bohemian national history was deprived during the restoration of the traces of its later rich life. It was artificially clothed into the garment of the 19th century but its interiors with costly paintings have remained mostly intact and represent thus the largest treasure of Gothic religious paintings in the whole world.

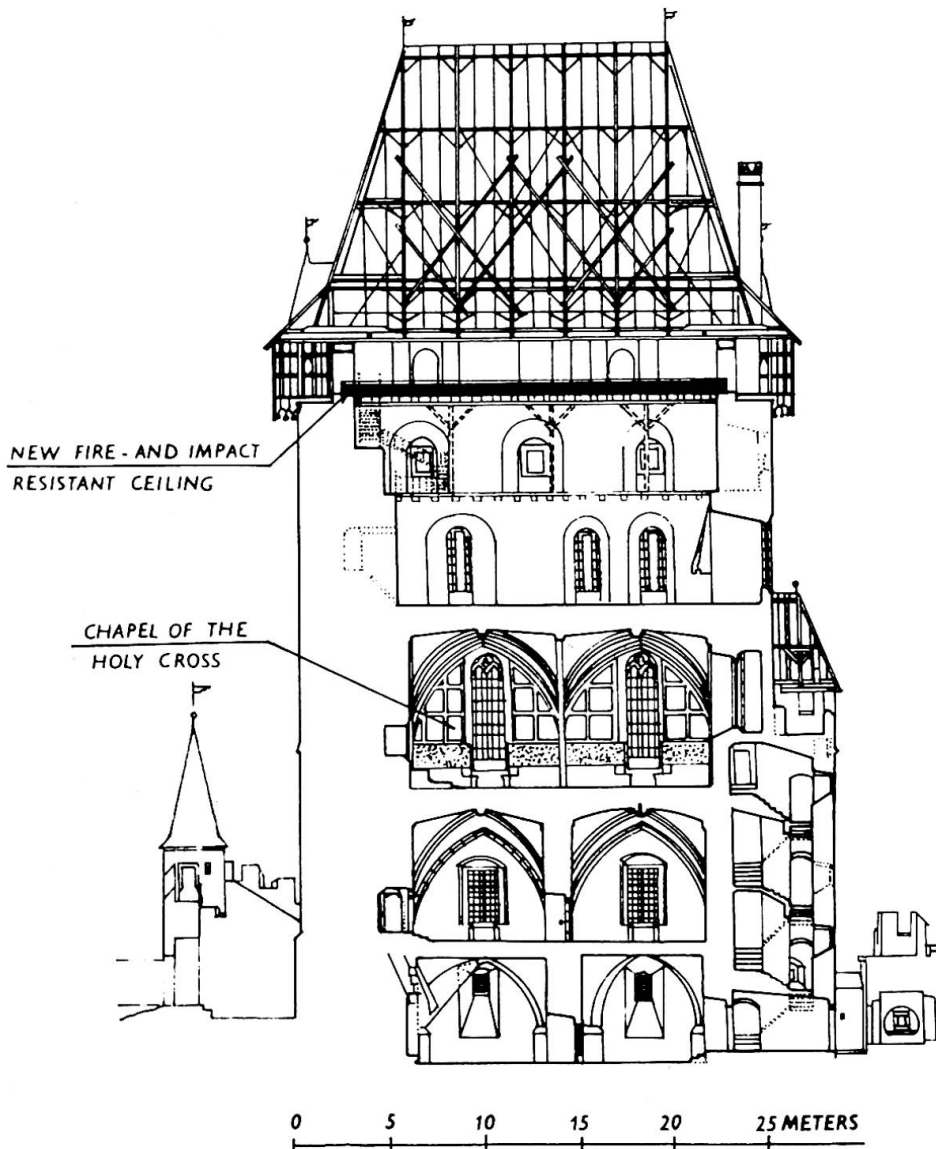
Lately it was decided to protect these paintings against the danger of fire and collapse of the 18 meters high roof trusses erected during the last reconstruction

at the end of 19th century. Design of fire- and impact- resistant ceilings, prepared by the author together with Mr. J. Bělohávek, M.Sc., C.E., will be briefly shown in this paper.

## 2. Purpose and Construction of the Fire- and Impact- Resistant Ceilings

The organisations of state care of historical monuments of Czechoslovak Socialist Republic decided that two fire- and impact- resistant ceilings have to be build on Karlštejn, protecting the Chapel of the Holy Cross and the Chapel of Virgin Mary from fire and collapse of roof trusses. Both these ceilings are designed in the loft level /Fig. 3/, having three main purposes:

- to protect the lower floors under loft from fire which could possibly be caused by a thunder-bolt or other reason
- to shield the ceilings in lower floors from destroying caused by collapse of the burning wooden roof trusses
- and to prevent the lower floors from drenching through with liquids used to extinguish the fire.



During the construction of these new ceilings no surcharge of old roof structures with low bearing capacity was permitted. As can be seen the task was rather complicated in every respect, in particular taking into account the dynamic forces acting simultaneously with very high temperature, reaching more than  $1200^{\circ}\text{C}$ . Solution of this problem was given by the author in form of a sandwich plate, where the upper layers have a heat insulation function damping at the same time the effects of impact. According to the thermal analysis in the first phase the roof crating with slate covering will be destroyed, falling all over the surface of the ceiling nearly at the same time. A protective net supported by cables anchored in

Fig. 3 Cross-section of donjon with position of the new ceiling

a special steel structure was designed to take this first dynamic load, falling down from the height of more than 15 meters and having a weight of nearly 40 Mp. This collapsed steel structure together with the ruins of the roof crating

will form another damping layer retaining the impact effects of falling heavy parts of the roof truss.

The main part of the new ceiling is formed by a reinforced concrete plate /Fig. 4/ of variable thickness placed on the outer bearing stone walls. As surcharge of old ceilings was not permitted it was designed to demolish the present brick paving with filling on the loft and to use the old battens as a formwork for the new ceiling. Both thermal and waterproofing insulation was proposed to be used on the lower surface, too, and in the lower room a steel centering was designed, taking the weight of the concrete placed in the first phase. The weight of the largest part of the

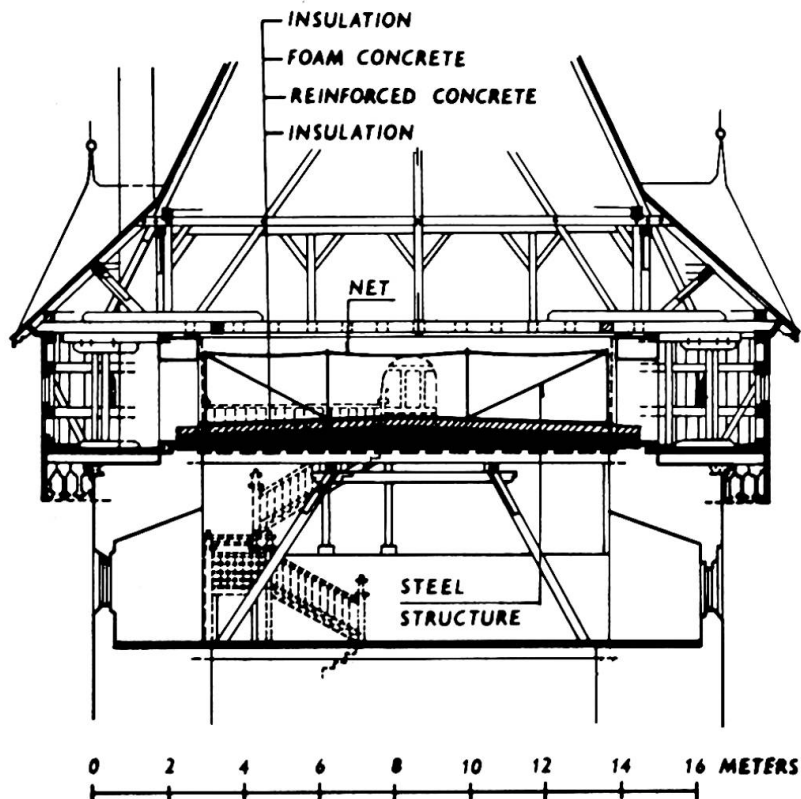


Fig. 4 Location and structural layers of the new designed ceiling

new ceiling is carried by this first - step reinforced concrete structure which is concreted in an elevated position so that no load acts on the wooden old structure.

### 3. Thermal and Dynamic Analysis

The thermal analysis was made by Mr. V. Reichel, M.Sc., C.E., as a basis for the next dynamic and static design and basic considerations. The full cubic contents of the roof truss and the crating is about  $110 \text{ m}^3$  of wood and the floor space among the outer bearing walls is  $221 \text{ m}^2$ . The results of the thermal analysis are as follows:

- the collapse of the roof crating will take place at about 20 minutes from the time when the fire starts
- the full breakdown of roof truss will last about 90 minutes
- the weight of the falling parts of the roof truss will be about a fourth part of the original weight, which is due to burning
- the temperature history during the fire on the top of the fire-resistant ceiling as calculated is shown in Fig. 5
- the relationship between fire duration and temperature in the concrete slab when no upper heat insulation layers were assumed shows Fig. 6.

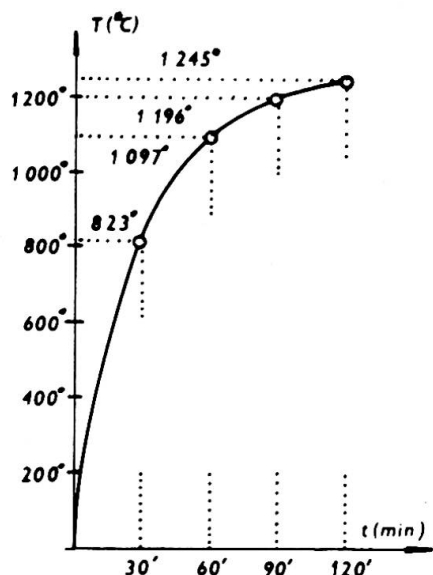


Fig. 5 Calculated temperature history during the fire

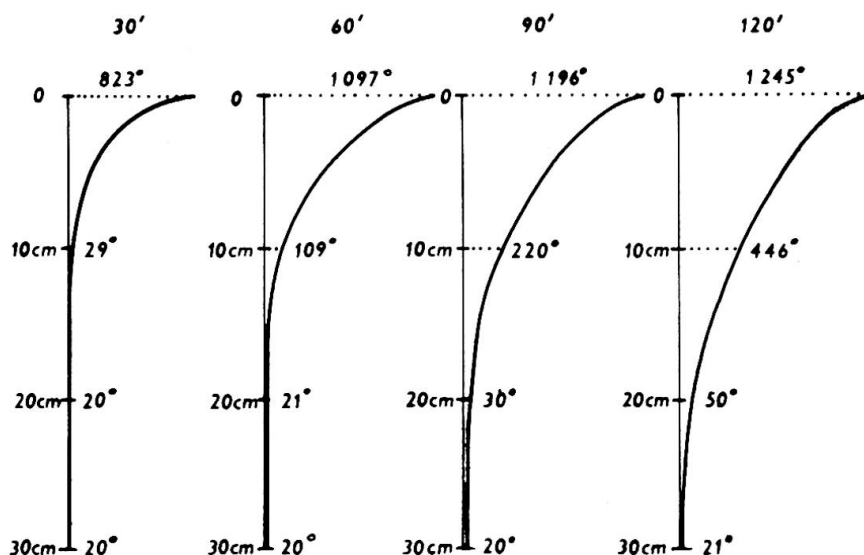


Fig. 6 Relationship between fire duration and temperature in the concrete without heat insulation layers

The dynamic analysis was made by Mr. Z. Podráský, M.Sc., C.E., in the way shown by Koloušek /5/ and on the basis of the results of thermal analysis. In the present study only a simplified dynamic design took place, using an energy method with reduced mass of the slab calculated by means of net method. The impact factor was calculated from the expression

$$\delta \sim 1 + \sqrt{1 + \frac{2h}{v_0} \cdot \frac{1}{1 + \frac{G_{red.}}{G_0}}} \quad /1/$$

where are:

- $\delta \sim$ ..... impact factor
- $h$ ..... height of the free fall
- $v_0$ ..... statical deflection of the slab due to the load  $G_0$
- $G_{red.}$ ..... reduced mass of the slab
- $G_0$ ..... the mass of the falling part of the roof truss

The damping was considered in this design approximately by reducing the height and mass of the falling parts of the roof truss which cannot be, however, determined precisely. The value of the impact factor calculated in this way was 6,2.

#### 4. Conclusion

The design of the fire- and impact- resistant ceilings on the Karlštejn Castle proposed by the author - when accepted - shall be realized in the years 1977 - 78. As many problems dealt with are quite new - some of them formulated here for the first time - much effort must be exerted to come to a complex and satisfactory solution. It shall be not only a question of more precisely defined assumptions and detailed calculation but also a task of much work on construction



details, material transport and, last but not least, better understanding of the philosophy of construction of this grand medieval building.

## 5. References

1. Gustaferrero, A.H.: How to Design Prestressed Concrete for a Specific Fire Endurance, Introductory Report, IABSE 10th Congress, Tokio, 1976, Zürich 1975, pp. 141 - 155
2. Kordina, K. Bornemann, P.: Brandverhalten von Stahlbetonplatten, DAfSt Heft 181, Wilhelm Ernst & Sohn, Berlin 1966
3. Kordina, K. Klingsch, W.: Tragverhalten brandbeanspruchter Bauteile, Vorbericht, IVBH 10. Kongress, Tokio, 1976, Zürich 1976, s. 287 - 292
4. Dvořáková, V. Menclová, D.: Karlštejn /in Czech/, SNKLU, Prague 1965
5. Koloušek, V. a kol.: Stavebné konštrukcie namáhané dynamickými účinkami /in Slovak/, SVTL, Bratislava 1967

## SUMMARY

In the paper a design of fire- and impact-resistant ceilings on Karlštejn Castle is briefly described. In this medieval complex the largest collection of Gothic religious paintings in the whole world is deposited and the new ceilings have to protect this treasure against the danger of fire and collapse of the high wooden roof trusses erected during the reconstruction at the end of the last century. This complex problem was solved by designing a sandwich plate and some results of thermal and dynamic analysis of this structure are presented.

## RESUME

L'auteur décrit la conception des plafonds résistant aux chocs et à l'incendie du château de Karlštejn. Cette construction médiévale possède la plus grande collection au monde de peintures religieuses gothiques et il fallait protéger celle-ci contre le danger d'incendie et d'effondrement des poutres du plafond en bois datant du siècle dernier. Ce problème a été résolu à l'aide d'un panneau sandwich; quelques résultats de calculs thermiques et dynamiques sont donnés.

## ZUSAMMENFASSUNG

Der Entwurf von stoss- und brandsicheren Decken für Schloss Karlštejn wird vorgestellt. Dieses mittelalterliche Gebäude besitzt die grösste Sammlung gotischer Devotionsbilder der Welt; es war deshalb nötig diese gegen die Brand- und Zusammenbruchgefahr von Deckenholzträgern des letzten Jahrhunderts zu schützen. Das Problem wurde mit Sandwichplatten gelöst; einige Ergebnisse der thermischen und dynamischen Berechnung werden dargestellt.

## Considérations sur l'étude théorique du comportement à l'incendie des structures en béton armé

Theoretische Betrachtungen zum Brandverhalten von Stahlbetonbauten

Considerations on the Theoretical Study of Reinforced Concrete Structures under Fire

J.C. DOTREPPE

Chargé de Recherches au F.N.R.S.

Université de Liège

Liège, Belgique

R. BAUS

Professeur Ordinaire

### 1. INTRODUCTION.

Le calcul au feu des structures en béton armé est un problème très complexe. D'une part, l'étude de la propagation de la chaleur dans les éléments en béton est difficile, par suite de la grande massivité des sections droites et de la faible conductivité thermique du béton. D'autre part, le comportement des structures en béton armé est complexe, par suite de la fissuration et du comportement non linéaire du béton, celui-ci étant de plus fonction de la température. C'est pourquoi nous estimons que l'étude théorique de ce problème doit se faire à partir de techniques de calcul évoluées, telles que celles décrites dans le Rapport Préliminaire [1], [6].

Dans cet article, on présente un code de calcul basé sur la méthode des éléments finis, qui est particulièrement bien adaptée à la résolution de ce type de problème. Cependant, nous avons adopté une discrétisation plus poussée, de manière à prendre en compte les différences de comportement du matériau.

### 2. CALCUL DE L'EVOLUTION DE LA TEMPERATURE DANS LES ELEMENTS.

Le problème de la répartition de la température dans le béton a une importance considérable. En effet, si la distribution de la température est mal évaluée, le calcul de la résistance au feu sera automatiquement erroné.

Dans le Rapport Préliminaire [4], nous avons indiqué les méthodes utilisées pour résoudre ce problème. Dans le cas des structures en béton, il n'est pas possible de procéder aux mêmes simplifications que dans le cas des structures en acier [2], et il est nécessaire de recourir aux techniques numériques décrites dans la référence précitée.

En ce qui concerne les propriétés thermiques du béton, il faut noter que la conductivité thermique  $\lambda$  décroît avec la température. Des valeurs de 1,5 ou 1,6 kcal/m.h.°C sont couramment admises à 0°C, tandis qu'elles tombent à 0,8 vers 1000°C. Il faut cependant signaler que des expériences récentes effectuées à l'Université de Gand ont conduit à des valeurs de  $\lambda$  beaucoup plus élevées aux températures modérées (2,8 pour le béton de gravier). La dilatation thermique du béton  $\alpha$  augmente avec la température jusqu'à 400°C environ, puis elle ne varie plus guère. La capacité thermique  $c$  ne varie guère avec la température, sauf aux environs de 100°C, par suite des phénomènes endothermiques apparaissant à cette température. Néanmoins, il est assez malaisé de tenir compte de cette particularité dans un modèle mathématique.



### 3. CALCUL DE LA RESISTANCE AU FEU DES POUTRES EN BÉTON ARMÉ

Le code de calcul utilisé est basé sur la méthode des éléments finis (cfr. figure 1). Une discrétisation supplémentaire est obtenue en divisant l'élément de structure en petits éléments parallépipédiques (figure 2). Le comportement peut varier d'un élément à l'autre, ce qui permet de tenir compte des différentes hétérogénéités. On obtient alors une discrétisation très poussée, et la technique de calcul est assez proche de celle utilisée par le Professeur BRESLER et le "Fire Research Group" de Berkeley [1]

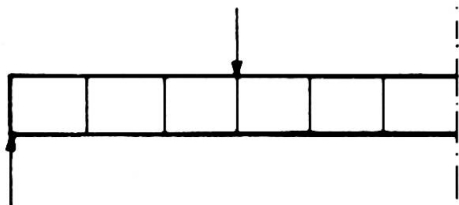


Figure 1

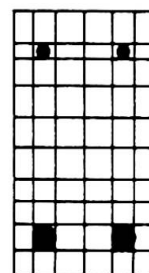


Figure 2

A partir des résultats fournis par l'étude thermique mentionnée au paragraphe précédent, il s'agit de calculer les déformations progressives de la poutre jusqu'au moment où l'on atteint la ruine par effondrement du système.

Deux phénomènes sont à la base de cette augmentation progressive des déformations :

- 1) L'augmentation de la température entraîne des effets thermiques qui dépendent fortement du mode d'appui de la poutre. Il faut noter que, dans le cas des structures en béton et contrairement à ce qui se produit pour les structures en acier, il existe toujours un gradient thermique important sur la section droite, par suite de la mauvaise conductivité thermique du béton.

S'il s'agit d'une poutre sur deux appuis simples, il apparaît des dilatactions thermiques importantes qui consistent en :

- un allongement de la pièce ;
- des déformations de flexion.

Ces déformations thermiques se font sans apparition de contraintes dans le matériau si la distribution de la température sur la section droite est linéaire ; dans le cas contraire, il y a toujours apparition de contraintes thermiques, mais celles-ci restent généralement assez faibles.

Si, au contraire, il s'agit d'une poutre biencastée, des contraintes thermiques importantes sont induites dans la structure, par suite de l'apparition de moments et d'efforts normaux de bridage aux appuis. Les déformations thermiques, par contre, restent faibles.

Dans le cas d'un élément isostatique, les calculs sont basés sur les formules de la thermoélasticité. Considérons une poutre de section quelconque, à comportement élastique, soumise à une distribution arbitraire de température sur la section droite. Les contraintes thermiques en un point d'ordonnée  $z$  sont données par la formule :

$$\sigma = -\alpha E \theta + \frac{P}{A} + \frac{Mz}{I} \quad (1)$$

avec  $A$  = aire transversale  
 $I$  = moment d'inertie  
 $\alpha$  = coefficient de dilatation thermique  
 $P$  et  $M$  ont pour expression :

$$P = \int_A \alpha E \theta dA \quad M = \int_A \alpha E \theta z dA \quad (2)$$



Figure 3

En ce qui concerne les déplacements dus aux effets thermiques, ils sont identiques à ceux de la même poutre soumise à une charge axiale  $P$  et à des moments d'extrémité  $M$ .

Dans le cas de la discrétisation envisagée, les formules précédentes doivent être modifiées, pour tenir compte du fait que les propriétés varient d'un point à l'autre en fonction de la température. Les expressions donnant  $P$  et  $M$  deviennent :

$$P = \sum_{i=1}^p \alpha_i E_i \theta_i A_i \quad M = \sum_{i=1}^p \alpha_i E_i \theta_i z_i A_i \quad (3)$$

où  $p$  désigne le nombre d'éléments parallélépipédiques.

Il faut noter ici que  $P$  et  $M$  ne sont pas rigoureusement constants le long de la poutre. De plus, comme le comportement du matériau n'est pas élastique, le calcul doit être fait pas à pas, en l'envisageant comme une succession de calculs élastiques.

- 2) L'augmentation de la température sur la section droite amène aussi une diminution des propriétés mécaniques du béton et de l'acier (résistance et module d'élasticité). Il en résulte que, sous charge constante, les déformations du système augmentent et la ruine se produit lorsqu'on dépasse la capacité portante de la poutre.

La prise en compte de ce phénomène ne présente pas trop de difficulté grâce à la discrétisation adoptée. En effet, la rigidité de chaque élément  $[K]$  est la somme des rigidités des  $p$  parallélépipèdes  $[K_i]$ . Chacune de ces rigidités dépend du module d'élasticité du matériau qui est fonction de la température  $E_i = E(\theta_i)$  : il diminue lorsque la température augmente. Il en résulte que les rigidités  $[K_i]$  diminuent, donc aussi la rigidité  $[K]$  de chaque élément et la rigidité globale de la structure.

Le calcul des rigidités est effectué par un procédé d'intégration numérique.

#### 4. EXEMPLE D'APPLICATION

Les propositions précédentes sont illustrées par un exemple de calcul. Il s'agit d'une poutre sur deux appuis simples qui a été testée au Laboratoire Herpol de l'Université de Gand. Les dimensions de la pièce et le mode de chargement sont indiqués à la figure 4, tandis que les dimensions transversales et la position des armatures sont données à la figure 5.

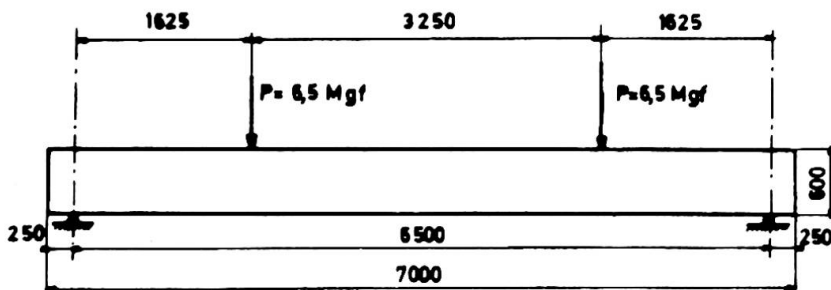


Figure 4

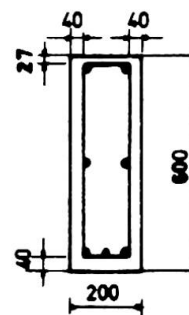


Figure 5

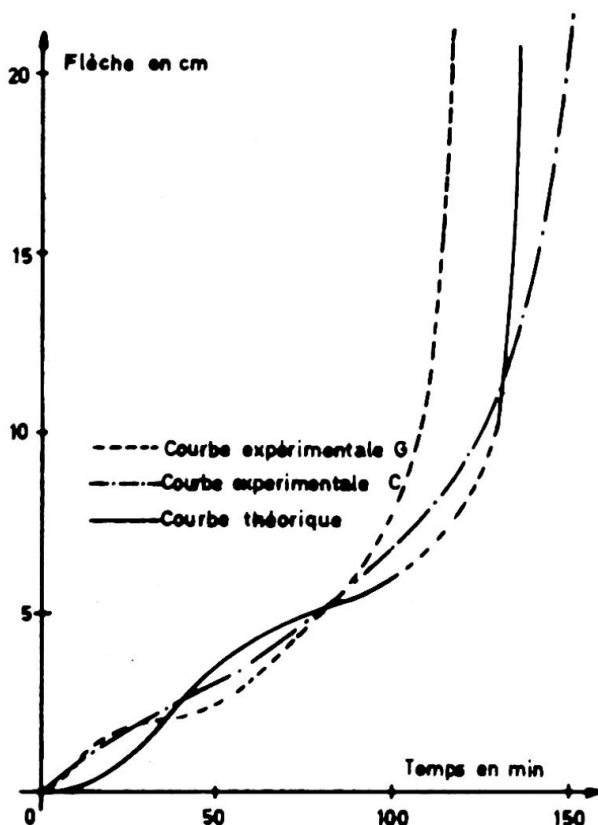


Figure 6

Une analyse par éléments finis a été réalisée pour la détermination de la distribution de la température (cf. [4]). On a noté une bonne concordance avec les résultats expérimentaux. La figure 6 donne l'évolution de la flèche en fonction du temps lorsque la température dans le four s'élève. Il y a deux courbes expérimentales, car deux types de béton ont été utilisés pour confectionner les poutres. On peut noter que les résultats obtenus avec notre modèle sont très satisfaisants.

#### 5. CONCLUSIONS.

Les considérations développées dans cet article montrent l'intérêt des méthodes numériques pour la prévision par le calcul du comportement à l'incendie des structures en béton armé. Les résultats obtenus pour les poutres isostatiques sont très encourageants.

En ce qui concerne les poutres hyperstatiques, des recherches sont actuellement en cours, car l'évolution des moments de bridage aux appuis semble dépendre fortement du fluage à chaud du béton.

#### BIBLIOGRAPHIE.

- [1] BRESLER, B. : Response of Reinforced Concrete Frames to Fire. Rapport Préliminaire, 10ème Congrès de l'AIPC, Tokyo, Septembre 1976. pp.273-280.
- [2] DOTREPPE, J-C. : Modèles Mathématiques pour le Comportement à l'Incendie des Structures. Séminaire UTI-CISCO "La Sécurité de la Construction face à l'Incendie", Saint-Rémy-lès-Chevreuse, Novembre 1975.
- [3] DOTREPPE, J-C. : Prévision par le Calcul du Comportement à l'Incendie des Structures Simples. Rapport de biennale (1973-1975) effectué dans le cadre des recherches de la Commission nationale belge "Recherche-Incendie", Service des Ponts et Charpentes, Liège, Mars 1976.
- [4] DOTREPPE, J-C, et HOGGE, M. · Détermination par la Méthode des Eléments Finis des Evolutions de Température pour les Structures Soumises à l'Incendie. Rapport Préliminaire, 10ème Congrès de l'AIPC, Tokyo, Septembre 1976, pp.213-218.
- [5] Méthode de Prévision par le Calcul du Comportement au Feu des Structures en Béton (D.T.U. Feu). Centre Scientifique et Technique du Bâtiment, Paris, Octobre 1974.
- [6] KORDINA, K., et KLINGSCH, W. : Tragverhalten Brandbeanspruchter Bauteile. Rapport Préliminaire, 10ème Congrès de l'AIPC, Tokyo, Septembre 1976, pp. 287-292.
- [7] PETTERSSON, O. : Theoretical Design of Fire Exposed Structures. Séminaire UTI-CISCO "La Sécurité de la Construction face à l'Incendie", Saint-Rémy-lès-Chevreuse, Novembre 1975.

#### RESUME

On présente un modèle mathématique pour l'évaluation de la résistance au feu des éléments en béton armé. Ce modèle est basé sur la méthode des éléments finis, mais une discrétisation plus poussée est utilisée pour prendre en compte les différences de comportement des matériaux. Les résultats obtenus pour les poutres isostatiques sont très encourageants.

## ZUSAMMENFASSUNG

Man stellt ein mathematisches Modell zur Untersuchung des Feuerwiderstandes von Stahlbetonelementen vor. Dieses Modell stützt sich auf die Methode der finiten Elemente; man benützt aber eine feinere Einteilung, um die Unterschiede im Materialverhalten berücksichtigen zu können. Für einfache Balken sind die erreichten Ergebnisse vielversprechend.

## SUMMARY

A mathematical model is presented for the evaluation of the fire resistance of reinforced concrete elements. This model is based on the finite element method, but a more refined discretization is used to take into account the various material behaviours. The results obtained for isostatic beams are very promising.

### IIIc

#### Rôle de l'eau libre dans le béton soumis au feu

Wirkung des Freiwassers im brandbeanspruchten Beton

Action of Free Water in Concrete under Fire

MICHEL ADAM

Directeur de la Réglementation

U.T.I.-F.N.B.T.P.

Paris, France

L'eau joue un rôle considérable dans le comportement des ouvrages en béton face au feu : on lui attribue aussi bien les éclatements qui peuvent conduire à la ruine que d'importantes absorptions de chaleur dues à la vaporisation qui permettent de prolonger de manière considérable la tenue au feu.

Tout dépend de la manière dont est répartie l'eau libre et de la manière dont elle pourra se vaporiser.

#### 1. ETUDES EN COURS.

Peu d'études systématiques ayant été publiées à ce jour, nous avons entrepris trois séries de recherches :

1.1. L'une sur des dalles homogènes de 7 et 12 cm d'épaisseur soumises dans leur plan à une contrainte axiale de 80 daN, variant par :

- la nature des granulats (calcaire, silico-calcaire, siliceux),
- le rapport eau/ciment (0,40 - 0,65),
- la répartition et la nature des armatures (acier doux  $\emptyset$  20 - acier mi-dur  $\emptyset$  6 et 20).

1.2. L'autre sur des dalles composées d'une prédalle de 5 cm associée à 6 à 9 cm de béton coulé en place.

1.3. La troisième sur des teneurs en eau réelles des ouvrages en service.

#### 2. AVANCEMENT DES TRAVAUX.

Les difficultés de réalisation de cette dernière recherche font que nous en sommes encore dans la phase préparatoire, par contre les deux premières nous ont déjà apporté des résultats intéressants, encore partiels (achèvement prévu dans un an), dont voici les grandes lignes :

##### 2.1. Essais d'éclatement sous contrainte axiale.

Essai selon la courbe ISO effectué à partir de juin 1976 sur des dalles de 1,5 x 0,8 m âgées de 90 jours (figure 1).

Le hasard a voulu que les mois de juin et juillet 1976 aient été en France particulièrement secs aussi, lors des essais, l'eau libre était évaporée dans les proportions ci-dessous :

Epaisseur	PERTES EN POIDS en % du poids total à 90 jours			
	7 cm		12 cm	
Rapport initial eau/ciment	0,40	0,65	0,40	0,65
à 90 jours	1,44	1,65	1,07	1,26
pendant l'essai	3,00	2,88	2,33	2,27

pour les dalles constituées avec des granulats silico-calcaires du Bassin Parisien. Parmi celles-ci, une seule dalle a éclaté et ce, dans sa partie armée (les dalles sont armées sur la moitié de leur surface); ses caractéristiques étaient :

- épaisseur : 12 cm - e/c = 0,65 - acier Tor 6 mm (maille 10 x 15 cm) -

Nous avons noté :

2,11. A propos des déformations longitudinales (figure 2), qu'à durée égale :

- les dalles non armées se raccourcissent rapidement en prenant de la courbure,
- de même, les dalles se raccourcissent dès qu'il y a éclatement si elles sont armées,
- les dalles gâchées les plus sèches paraissent les plus rigides, et ce d'autant plus que l'armature est grosse et que la dalle est mince,
- le palier de dilatation est obtenu pour une température d'environ 275°C pour l'acier doux et 350°C pour l'acier écroui à froid.

2,12. A propos de la température des aciers (figure 3), qu'à durée égale :

- il y a un gain compris entre 40°C et 70°C quand l'épaisseur passe de 7 à 12 cm (il n'y a pratiquement pas de palier à 100°C pour 7 cm d'épaisseur), mais qui peut être plus fort du fait que si les aciers sont de plus gros diamètre, l'enrobage est plus important.
- il existe un gradient d'environ 70°C entre la génératrice inférieure et la génératrice supérieure des aciers de 20 mm (acier lisse ou non), et les températures sont du même ordre sur les aciers lisses et sur les aciers à adhérence améliorée,
- le rapport e/c joue à peine pour les dalles de 7 cm, mais permet de gagner environ 100°C pour les dalles de 12 cm.

2,2. Essais de prédalles (Figure 4).

Les dalles ont 4 x 1,8 m et sont chargées à 250 kg/m<sup>2</sup>. Les prédalles ont toutes 5 cm d'épaisseur, le béton coulé en place 6 cm en général.

Dès à présent, il convient d'insister sur l'importance que revêt la prédalle.



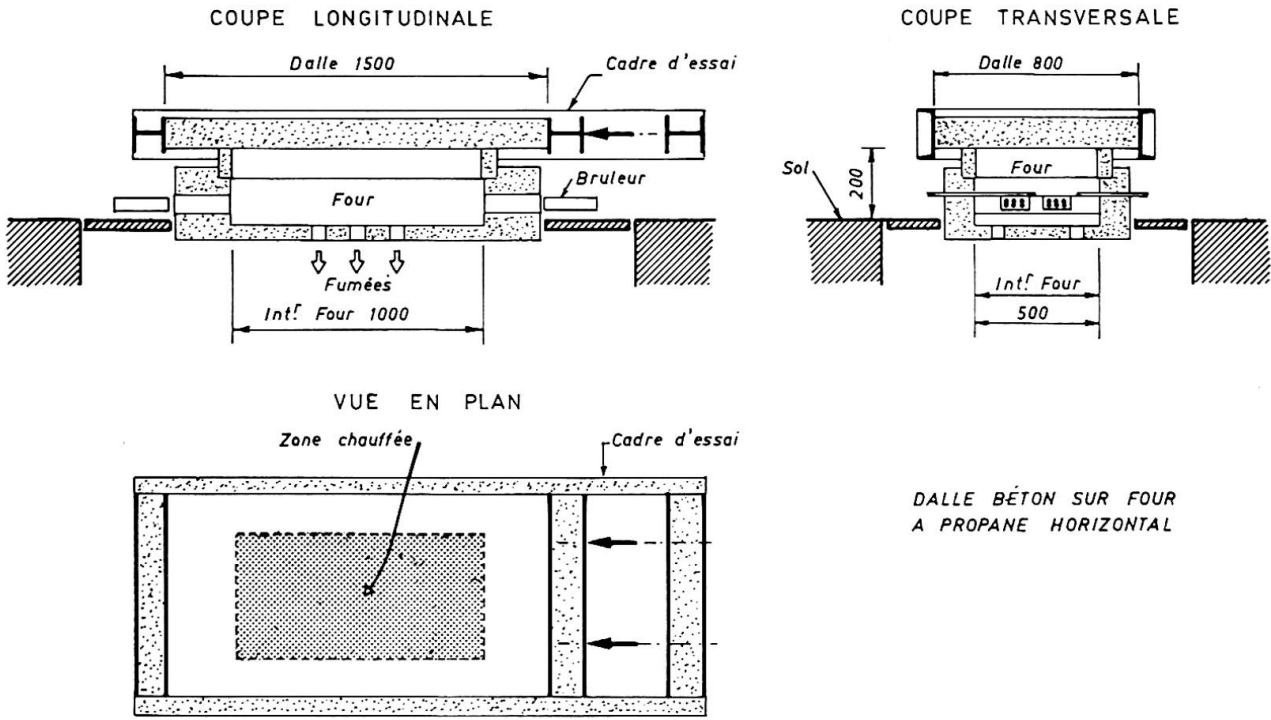
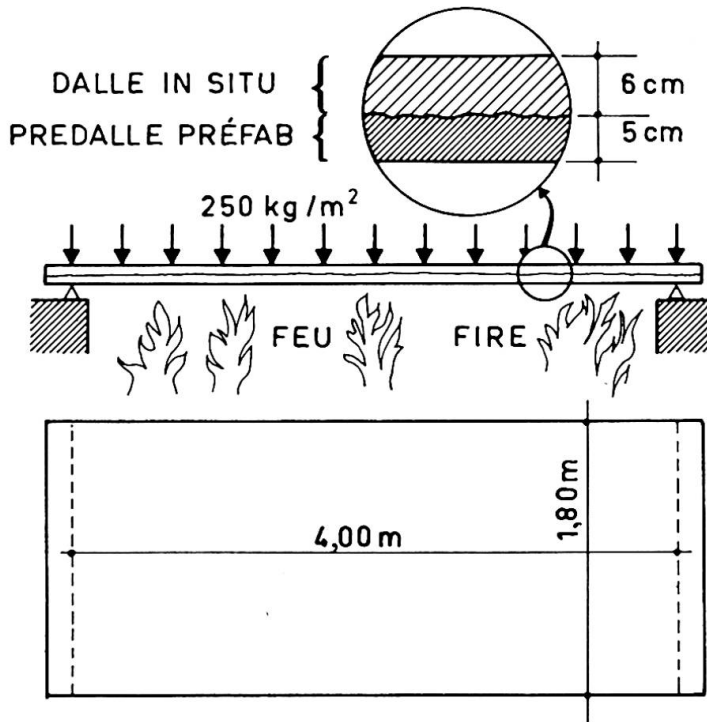
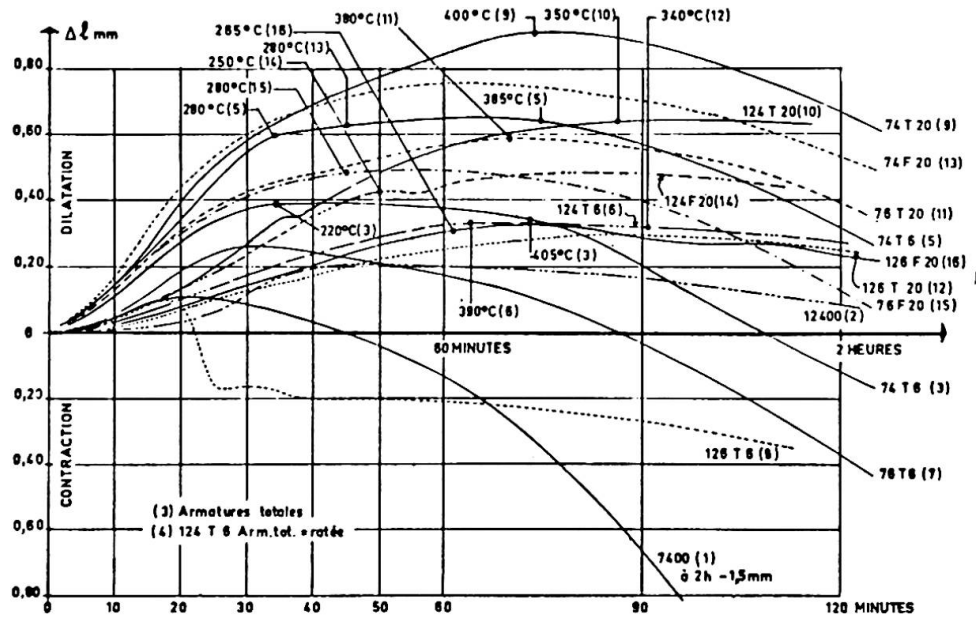


Fig. 1.- Schéma des dalles comprimées axialement et du dispositif d'essais.





28.7.76 ESSAIS ÉCLATEMENTS CHAMPS SUR MERNE.

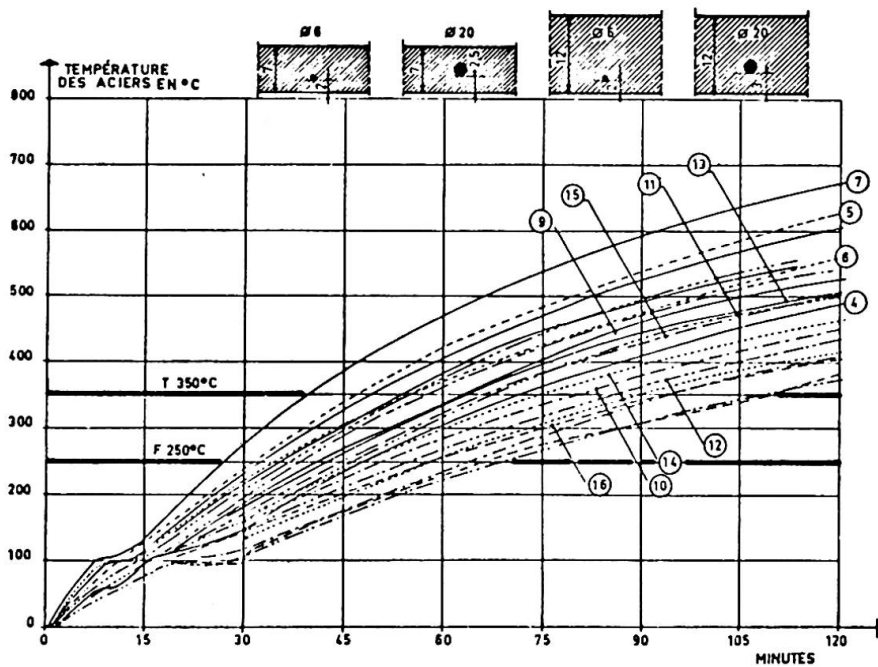


Fig. 2 et 3.- Essais d'éclatements de dalles comprimées axialement.  
Dilatation axiale et température des aciers :

- premier nombre (7 - 12) : épaisseur en cm
- deuxième nombre ( 4 :  $e/c = 0,40$   
                          ( 6 :  $e/c = 0,65$
- troisième nombre ( T 6 : acier écroui  $\varnothing$  6 mm  
                          ( T 20 : acier écroui  $\varnothing$  20 mm  
                          ( F 20 : acier doux  $\varnothing$  20 mm

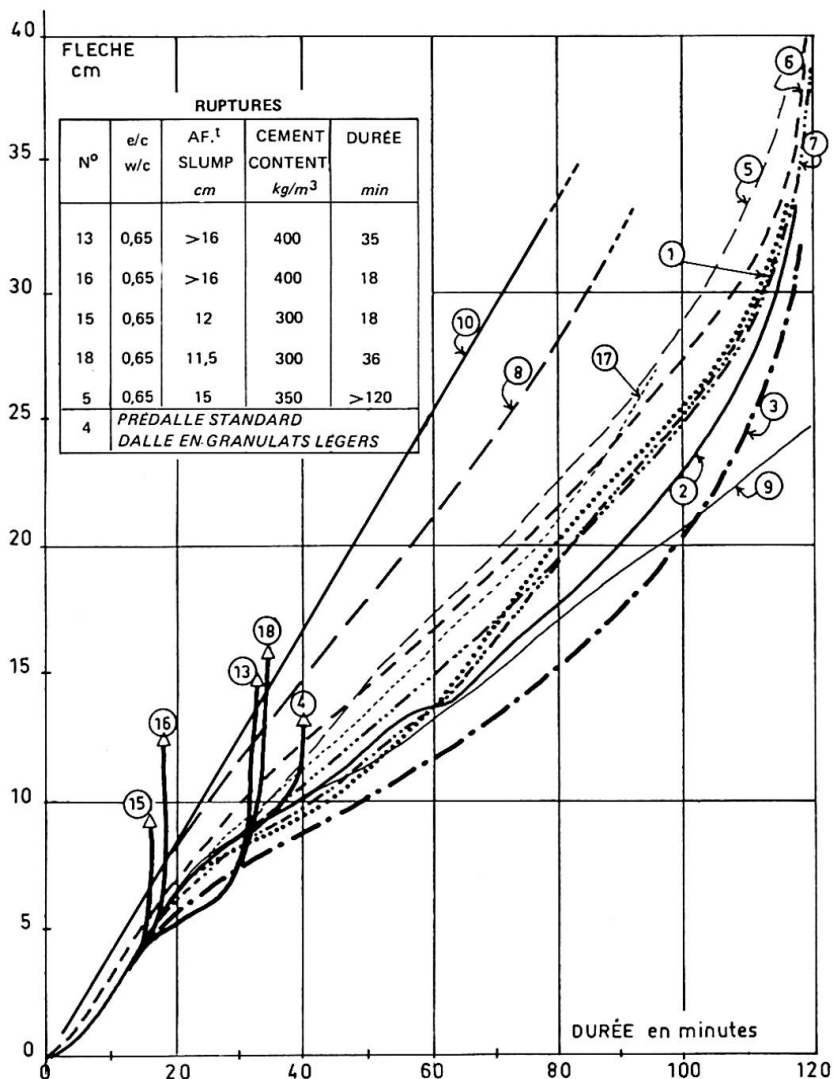


Fig. 5. Essais de prédalles (bi-couches) : Mesure des flèches.

Repérage des échantillons :

1. Élément standard.

- ( prédalle : 5 cm - silico-calcaire - e/c = 0,45 - moule vibrant -  
350 kg/m<sup>3</sup> de CPA 400 étuvé à 60°C - armature Ø 12 tous les 19 cm.
- ( dalle : 6 cm - silico-calcaire - e/c = 0,50 - aiguille vibrante -  
350 kg/m<sup>3</sup> de CPAL 325 non chauffé.

Repère	Autres échantillons	Paramètre
2. 3.	prédalle = 0 cm, dalle = 11 cm prédalle = 5 cm, dalle = 9 cm	) épaisseur
5. 6. 7.	prédalle non vibrée (e/c = 0,65) prédalle aiguille vibrante (e/c = 0,45) prédalle moule vibrant (e/c = 0,45)	) Mode de serrage
4. 8. 9. 10.	prédalle = 5 cm, dalle = 11 cm de granulats légers prédalle granulats silico-calcaires prédalle granulats calcaires prédalle granulats siliceux	) Type de granulats
11. 12.	prédalle - armature Ø 16 tous les 33 cm prédalle - armature Ø 8 tous les 9 cm	) Armature
13. 14. 15. 16. 17. 18.	Dalle e/c = 0,50 Prédalle 400 kg/m <sup>3</sup> de CPA 400 e/c = 0,65 ) " e/c = 0,50 " 300 kg/m <sup>3</sup> de CPA 400 e/c = 0,45 ) " e/c = 0,50 " 300 kg/m <sup>3</sup> de CPA 400 e/c = 0,65 ) Dalle e/c = 0,65 Prédalle 400 kg/m <sup>3</sup> de CPA 400 e/c = 0,65 ) " e/c = 0,65 " 300 kg/m <sup>3</sup> de CPA 400 e/c = 0,45 ) " e/c = 0,65 " 300 kg/m <sup>3</sup> de CPA 400 e/c = 0,65 )	) Ciment et e/c

Ainsi nous avons constaté (figure 5) :

- à un dosage en ciment portland de 350 kg/m<sup>3</sup>, une prédalle non vibrée à la fabrication entraîne des flèches importantes à partir de la première heure et la ruine après 2 heures lors du refroidissement ;
- le type de granulat utilisé pour la prédalle joue un rôle important : ainsi pour atteindre une flèche de 1/30e, le temps est passé de 30 minutes à une heure lorsque l'on remplace la silice par du calcaire ;
- quel que soit le dosage (300 ou 400 kg/m<sup>3</sup> de ciment portland), un rapport eau/ciment de 0,65 entraîne une rupture brutale très rapide au cours de la première demi-heure de l'essai, alors que la sous-face est entre 260 et 300°C, les aciers entre 115 et 125°C, l'interface entre 60 et 90°C et la surface entre 18 et 20°C. La rupture s'explique par la désolidarisation complète à l'interface ;
- une surface d'accrochage insuffisamment rugueuse constitue un chemin préférentiel pour l'eau, et si certaines zones lisses sont entourées de parties rugueuses, cela peut provoquer un décollement brutal des deux couches.

D'ici un an, nous pourrons grâce en partie à ces résultats compléter le règlement actuellement en vigueur en France concernant le calcul des ouvrages au feu (D.T.U. "Méthode de prévision par le calcul du comportement au feu des structures en béton").

#### RESUME

L'intervention traite du rôle de l'eau libre se trouvant dans le béton au moment de l'incendie dans les deux cas suivants:

- Dalles homogènes de 7 et 12 cm soumises à une contrainte de compression unidirectionnelle dans leur plan de 80 daN,
- Dalles isostatiques constituées de 2 couches de béton d'âges différents chargées uniformément.

Les recherches en cours montrent l'incidence sur la température des armatures et leur comportement selon qu'il s'agit d'aciers doux ou écrouis, l'importance d'un dosage suffisant en béton (350 kg/m<sup>3</sup>), de la qualité de la mise en oeuvre et de la qualité de la liaison entre les deux couches de béton.

#### ZUSAMMENFASSUNG

Der Artikel behandelt die Wirkung des Freiwassers im Beton unter Brandbeanspruchung in den zwei folgenden Fällen:

- Homogene Platten, 7 und 12 cm stark, die einer eindimensionalen Druckspannung von 80 daN in ihrer Ebene unterworfen sind,
- Statisch bestimmte Platten unter Gleichlast, die aus einem 5 cm starken vorgefertigten Element und einem Aufbeton bestehen.

Die laufenden Untersuchungen zeigen den Einfluss der Bewehrungen auf die Temperatur und ihr Verhalten je nachdem, ob es sich um naturharten oder um kaltverformten Stahl handelt, die Bedeutung einer genügenden Zementdosierung (350 kg/m<sup>3</sup>), die Verarbeitungsgüte und die Güte der Haftung zwischen den beiden Betonlagen.

#### SUMMARY

The paper concerns the action of free water in concrete during a fire into the following cases:

- Uniform slabs of 7 and 12 cm thickness submitted to an axial load in their own plan of 800 N,
- Isostatic slabs formed by a layer of concrete poured in situ on a precast 5 cm thin slab with uniform loading.

The investigation in progress shows the action of the reinforcing bars on the temperature and on their behaviour in relation with the type of steel bars, the importance of the cement contents (more than 350 kg/m<sup>3</sup>), of the water/cement ratio, and of the good quality of the bonding between the two concrete layers.

**Spalling of Concrete in Actual Fire**

Eclatement du béton dans un incendie réel

Ausplatzen von Beton bei einem echten Brand

**K. SHIRAYAMA**

Director

**F. TOMOSAWA**

Section Chief

**K. KAWASE**

Section Chief

Building Research Institute, Ministry of Construction

Tokyo, Japan

Spalling experiment conducted with fifty-two 1m x 1m test panels of reinforced concrete has shown a prominent effect of free water in concrete on spalling phenomenon of both lightweight and ordinary aggregate concrete, as we have reported in the preliminary report. The result shows that spalling is liable to occur when the amount of free water in concrete is increased above the range of 120 to 130kg per cubic meter of concrete. 1)

Fig. 1 and fig. 2 show the examples of test panels exposed to fire. The test panel in fig. 1 made of ordinary aggregate concrete and having 140kg/m<sup>3</sup> of free water shows a remarkable spalling, while the panel in fig. 2 made of lightweight aggregate concrete shows a slight spalling on the exposed surface, the amount of free water being 120kg/m<sup>3</sup>.

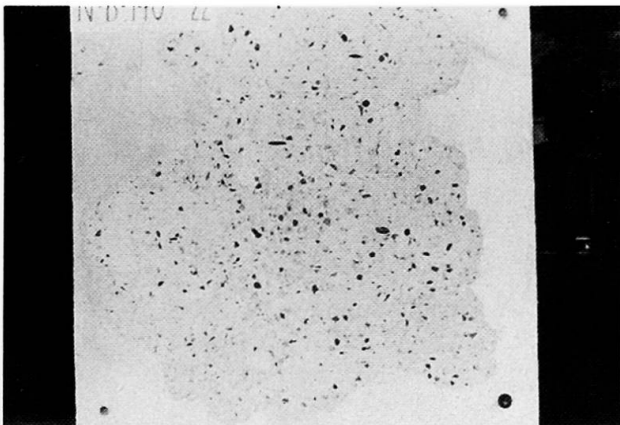


Fig.1

Ordinary aggregate concrete test panel  
having 140 kg/m<sup>3</sup> of free water

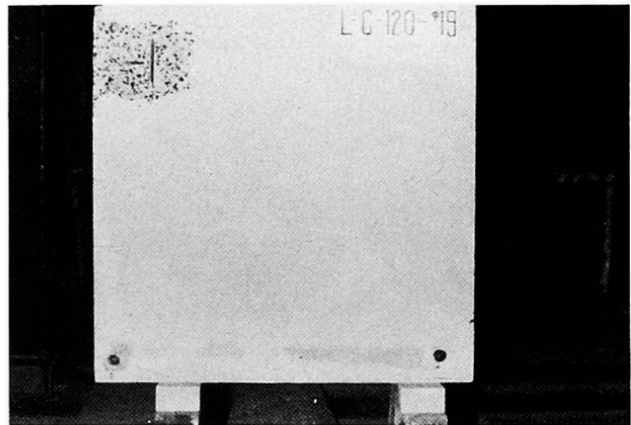


Fig.2

Lightweight aggregate concrete test panel  
having 120 kg/m<sup>3</sup> of free water

An investigation is now under consideration to make clear what amount of free water exists in realized concrete structures. A preliminary study for this investigation on the loss of free water from  $\phi 15 \times 30$ cm cylinder made of lightweight aggregate concrete in the course of atmospheric drying in the room shows that lightweight aggregate concrete has about 100 to 120kg/m<sup>3</sup> of free water at the age of 3 months, and the amount of free water of air dried concrete seems to be in equilibrium within this level (fig. 3).

We can consider that the amount of free water in the lightweight aggregate concrete in realized structures also decreases to this level after the age of 3 months or more, according to the size and exposure conditions of the concrete elements. For ordinary concrete, the initial and the equilibrium amount of free water is less than those for lightweight aggregate concrete.

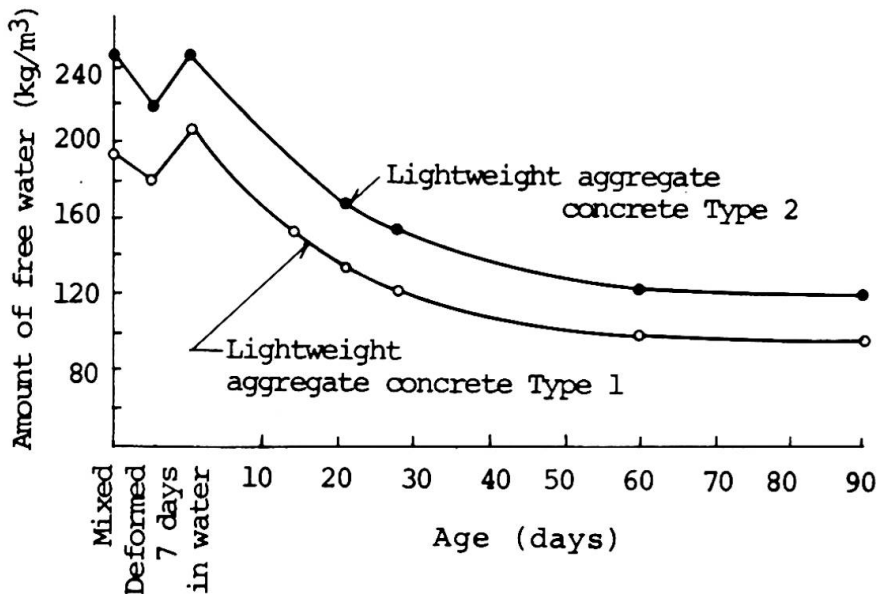


Fig. 3 Loss of free water from lightweight aggregate concrete ( $\phi 15 \times 30$  cylinder)

The following are some examples of spalling phenomenon in actual fire which seem to represent different levels of the amount of free water and different types of aggregate used. The examples are limited but we could recognize an effect of the amount of free water in concrete on spalling in actual fire, as in the experiment.

**Example 1: Explosive Spalling Occurred in Fire of a Reinforced Concrete Structure Building under Construction**

This example, reported by K. Kizawa and S. Ohgishi in 1967, shows a remarkable spalling in concrete during hardening. A five-story reinforced concrete shop building having 2,200m<sup>2</sup> total floor area was under construction when fire spread from the 3rd to the 5th floor, 5 days after concreting in the 4th story and floor slab of the 5th story. It was 17th day after concreting in the 3rd story.

Spalling was so much intensive as to be explosive at the 5th story floor slab and at the bearing wall around the elevator shaft in the 3rd and 4th story. The concrete was of ordinary aggregate

and the amount of free water should have been very high because of early ages of concrete (fig. 4).



Fig.4  
Spalling at the wall of the  
elevater shaft

Example 2: Spalling in Fire of a Reinforced Concrete and Steel Structure Building Nearing Opening

The building was a six-story steel structure with a basement of reinforced concrete, having 60,000m<sup>2</sup> total floor area. The floor slab of each story was of reinforced lightweight aggregate concrete except that ordinary aggregate concrete was used in the basement.

Fire occurred at the basement, just before the opening of the building, spread from the 2nd to the 4th floor, the 1st floor remaining undestroyed, and continued for 15 hours smoldering. It was about 6 months after concreting.

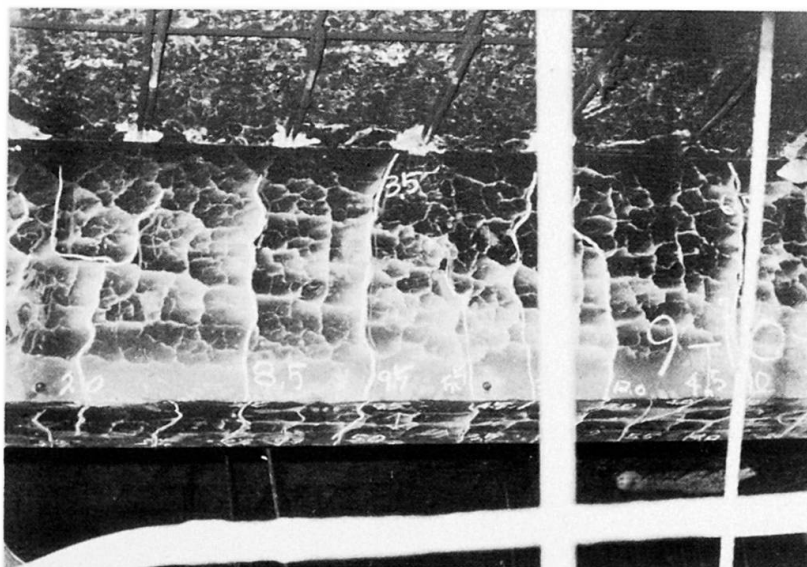


Fig.5  
Spalling at the under side of floor slab



Spalling of concrete was observed at the under side of each floor slab and at the reinforced concrete beam and girder of the basement. It was so much remarkable in severely attacked slabs that the lower reinforcing bars of the slabs were entirely bared out (fig. 5).

It was considered that the cause of this remarkable spalling could be a fairly high content of free water in the concrete, especially in that of the basement, and the long duration of fire due to the abundance of combustibles.

**Example 3: Spalling in Fire after Gas Explosion of a Precast Concrete Structure Apartment House**

The building was of a composite structure of H section steel frame and precast concrete large panels. The large panels were made of lightweight aggregate concrete and manufactured by steam curing. Fire occurred after gas explosion in an apartment on the 6th floor and spread to adjoining 5 apartments.

Though the damage by the gas explosion was so heavy as to destroy the walls and slabs (fig. 6), spalling was observed only at the lower corner of the beams and around the ventiration opening penetrating them (fig. 7). The cause of the slight spalling might be a fairly low content of free water in the concrete due to steam curing.

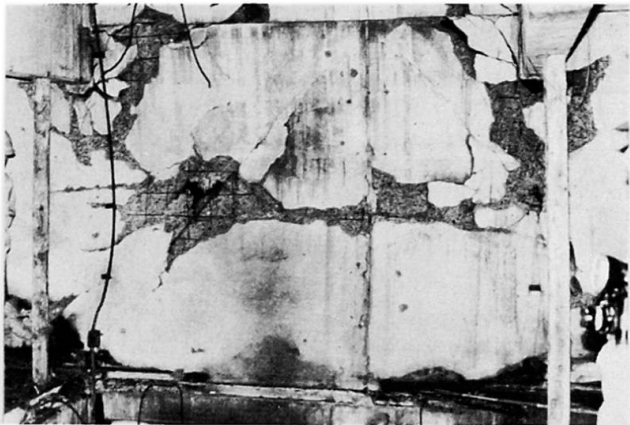


Fig.6  
A wall destroyed by gas explosion



Fig.7  
Spalling at the beam

**Example 4: Spalling in Fire of a Reinforced Lightweight Aggregate Concrete Apartment House**

The apartment house is of a composite structure of lightweight aggregate concrete cast-in-situ, having 11 stories. Fire occurred in March 1976, i.e. 6 years after completion, in an apartment on the 8th floor and this apartment was fully burnt out.

Spalling could scarcely be observed except at the under side of balcony slab of the upper story. The spalled part was about 80cm x 50cm, depth about 2cm, and its appearance was as same as that of test panels spalled in our experiment. This part has been attacked directly by the flame going out from the broken window, and the amount of free water in the slab should have been higher than in interior elements (fig. 8).

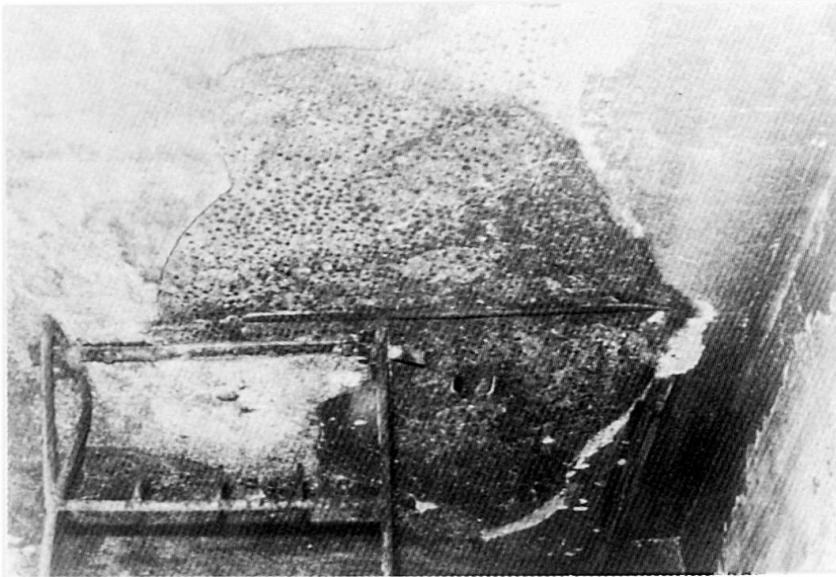


Fig.8

Spalling at the under side of balcony slab

#### SUMMARY

Four examples of spalling of concrete in actual fire representing different levels of the amount of free water and different types of aggregates used are shown. An effect of the amount of free water in concrete on spalling could be significant in actual fire as in the experiment, the amount of free water in realized concrete structures being to be investigated.

#### RESUME

On présente 4 exemples d'éclatement du béton dans un incendie réel, avec des bétons correspondant à différentes quantités d'eau libre et à des agrégats différents. L'effet d'une certaine quantité d'eau libre pourrait être déterminant pour l'éclatement du béton, dans des incendies réels comme en laboratoire, mais il reste à déterminer la quantité d'eau libre se trouvant en réalité dans le béton des structures existantes.

#### ZUSAMMENFASSUNG

Vier Beispiele des Ausplatzens von Beton bei einem echten Brand werden gezeigt; die Betons werden mit verschiedenen Mengen Freiwasser und mit verschiedenen Aggregaten vorbereitet. Die Wirkung einer gewissen Menge Freiwasser auf das Ausplatzen des Betons könnte sowohl bei wirklichen Bränden wie auch im Labor entscheidend sein, es wäre aber noch notwendig, die Menge Freiwasser im Beton von bestehenden Bauwerken festzustellen.

Leere Seite  
Blank page  
Page vide